Nanoscale

Accepted Manuscript

This article can be cited before page numbers have been issued, to do this please use: Y. Fan and M. Chen, *Nanoscale*, 2025, DOI: 10.1039/D5NR00938C.

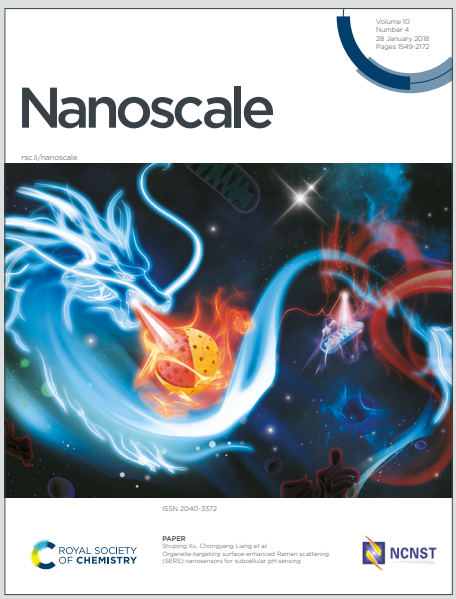

ROYAL SOCIETY OF CHEMISTRY

rsc.li/nanoscale

View Article Online
DOI: 10.1039/D5NR00938C

Emerging frontiers in chiral metal−organic framework membranes: diverse synthesis techniques and applications

*Yun Fan [a], Mengyun Chen [b,] **

a Key Laboratory of Flexible Electronics (KLOFE), Institute of Advanced Materials (IAM) & School of Flexible Electronics (Future Technologies), Nanjing Tech University, 30 South Puzhu Road, Nanjing 211816, China

b Department of Physics, Chemistry and Biology (IFM), Linköping University, Linköping, 58183 Sweden

Email: mengyun.chen@liu.se

Abstract

Chirality is one of the interesting isomers in nature. Chiral materials, in multiple forms, usually show unique physical phenomenon, such as chiral luminescence, and distinctive chemical properties. Metal−organic framework (MOF) membrane have high porosity and abundant active sites, thus is a perfect alternative for functionalization. With involvement of chiral unit, chiral MOF membranes show excellent applications for chiral sensing, separation and luminescence. In this review, we first introduce the up-to-date preparation methods of chiral MOF membranes, including direct and indirect methods, and then discuss their applications in enantiomers recognition, chiral separation, and circular polarization luminescence. Finally, we conclude the challenges in chiral MOF membranes and provide a perspective of future development.

View Article Online
DOI: 10.1039/D5NR00938C

1. Introduction

Metal-organic frameworks are a type of porous compounds formed by self-assembly of metal ions or clusters with organic ligands.[1-3] With the unique properties such as high porosity, large surface area, adjustable pore structure, and accessible active sites, MOFs have broad applications in separation, catalysis, sensing, and energy storage.[4,5] Research on MOF materials is gradually expanding from bulk materials to membrane materials, as membranes take advantage of low cost, low energy consumption and reusability, which are important for applications.[6-8]

Chiral molecules are interesting materials, showing unique physical phenomenon, such as chiral luminescence, and distinctive chemical properties, e.g. chiral materials share similar structures but possibly completely different physicochemical or biological properties properties.[9,10] For example, one enantiomer performs the desired function, while the other shows an inactive state or in some cases even cause unwanted side effects, which is significant in drugs and food safety, and chemical synthesis.[11,12]

Attributing to the abundant active sites on the MOFs, people achieved chiral MOFs by involvement of chiral units via various methods (e.g. adding chiral ligands, chiral secondary structural units, post modification, or chiral induction).[13-16] Based on chiral MOFs materials, researchers have developed chiral MOF membranes for practical applications.[17] With ordered pore structure by arrangement of crystal growth, chiral MOF membranes provide better recognition and separation of enantiomers, e.g. chiral drugs, chiral gas molecules.[18-20] By integrating fluorescent units, chiral MOF membranes present circular polarization luminescence (CPL), which are potential for applications in information storage, anti-counterfeiting, and encryption.[21] In all, Chiral MOF membranes, as an emerging functional material, have seen the great progress in preparation and applications, which inspire us to organize a review for the stage.

In this review, we first introduce the preparation of chiral MOF membranes, including direct methods (solvothermal synthesis, layer-by-layer synthesis (lbl), and template-assisted synthesis) and indirect methods (solution casting and thermally induced phase separation-hot pressing (TIPS-HoP)) (Fig. 1).[22-24] Then, we summarize the applications of chiral MOF membranes in chiral sensing, chiral separation, and CPL. Finally, we put forward our own insights into obtaining high-quality chiral MOF membranes for better applications.

View Article Online
DOI: 10.1039/D5NR00938C

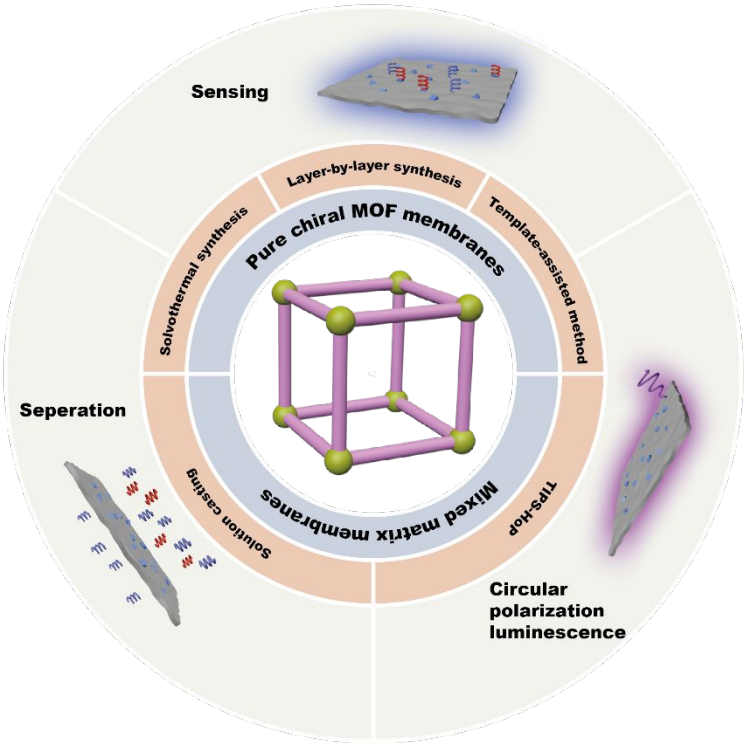

Fig. 1 Summary of preparation strategies and applications of chiral MOF membranes.

2. Preparation of chiral MOF membranes

There are the two main forms of chiral MOF membranes, pure membranes and MMMs, according to the existence of matrix. The direct methods are used for the synthesis of pure chiral MOF membranes, while the indirect methods are used for the synthesis of MMMs. The synthesis of pure chiral MOF membranes is simple, usually one step on the substrate. Self-supporting MMMs are prepared by the synthesis of chiral MOF materials and then the fabrication of membranes. Due to the mixture with various matrices, chiral MOF MMMs inherit their advantages of good mechanical stability and processability, which ensures simultaneous increase on permeability and selectivity.[25] We will discuss the methods for preparing pure chiral MOF membranes and MMMs in the following section.

2.1. Pure chiral MOF membranes

Pure chiral MOF membranes are synthesized from chiral MOF precursors by in-situ synthesis on substrates, including one-pot solvothermal synthesis, lbl synthesis, and template-assisted synthesis.

One-pot solvothermal synthesis. In this method, substrates are immersed into the chiral precursor solution, letting chiral MOF membrane to grow directly on them. This method is simple,

View Article Online
DOI: 10.1039/D5NR00938C

efficient, and ensures the high thermal stability of membranes. Anodic aluminum oxide (AAO) substrates are frequently used for the preparation of chiral MOF membrane. For example, Wang et al. reported the preparation of *l*-His-ZIF-8 membrane with good continuity through in-situ growth method.[19] The *l*-His-ZIF-8 membrane prepared by placing the AAO substrate horizontally in a precursor solution of Zn ions, Hmim, and *l*-His completely covered the AAO substrate and showed high integrity. The characteristic peaks of amino and carboxylic groups observed in the membrane indicated that *l*-His, as the ligand molecule, had been successfully incorporated into the ZIF-8 framework, endowing MOF with chirality and providing a chiral channel for the separation of enantiomers.

In addition, metal source substrates are usually used to prepare MOF membranes, which not only serve as substrates but also participate in the synthesis.[26] Qiu et al. prepared Ni_2(*l*-asp)$_2$(bipy) membrane on Ni net substrate by using solvothermal method with a thickness of 10-20 μm (Fig. 2a).[27] The Ni net was horizontally placed in the autoclave and reacted with a solution of 4,4'-bipyridine (bipy) and *l*-aspartic acid (*l*-asp) ligands. The Ni ions in the Ni net acted as anchoring active sites, coordinating with organic ligands to promote the nucleation and growth of MOFs. Ni_2(*l*-asp)$_2$(bipy) grew around the wires of Ni net, and then alternately grew to form a continuous Ni_2(*l*-asp)$_2$(bipy) membrane, creating strong adhesion between membrane and Ni net substrate. The thin and defect-free Ni_2(*l*-asp)$_2$(bipy) membrane was prepared using this single metal source method, as the formation of a layer of the membrane led to the cessation of growth process due to the absence of metal source. X-ray diffraction (XRD) and scanning electron microscopy (SEM) characterization indicated the high crystallinity and continuity of Ni_2(*l*-asp)$_2$(bipy) membrane.

In-situ secondary growth of MOFs on substrates is used to obtain continuous and well-intergrown MOF membranes. Recently, Zhao et al. synthesized chiral MOF-808 membranes on α-aluminum oxide (α-Al_2O_3) substrate through secondary growth and post-synthetic modification (Fig. 2b).[23] Firstly, the α-Al_2O_3 substrate was vertically placed in the precursor solution of MOF-808 for solvothermal reaction to prepare seeded MOF-808 membrane. Then, the membrane was placed in the precursor solution of MOF-808 for secondary growth to obtain the continuous MOF-808 membrane. Subsequently, the chiral MOF-808 membranes MOF-808-Ala, MOF-808-Thr, and MOF-808-His were grown after reacting in solutions of chiral molecules *l*-alanine (*l*-Ala), *l*-threonine (*l*-Thr), and *l*-histidine (*l*-His), respectively. The introduced amino acid molecules

View Article Online
DOI: 10.1039/D5NR00938C

partially replaced the trifluoroacetic acid regulator on the Zr cluster to coordinate with the unoccupied Zr cluster, thus being integrated into the MOF-808 structure. The chiral MOF-808 membranes obtained by post-synthetic modification retained the crystallinity of MOF-808, and their thicknesses could be controlled by regulating the concentration of metal ions.

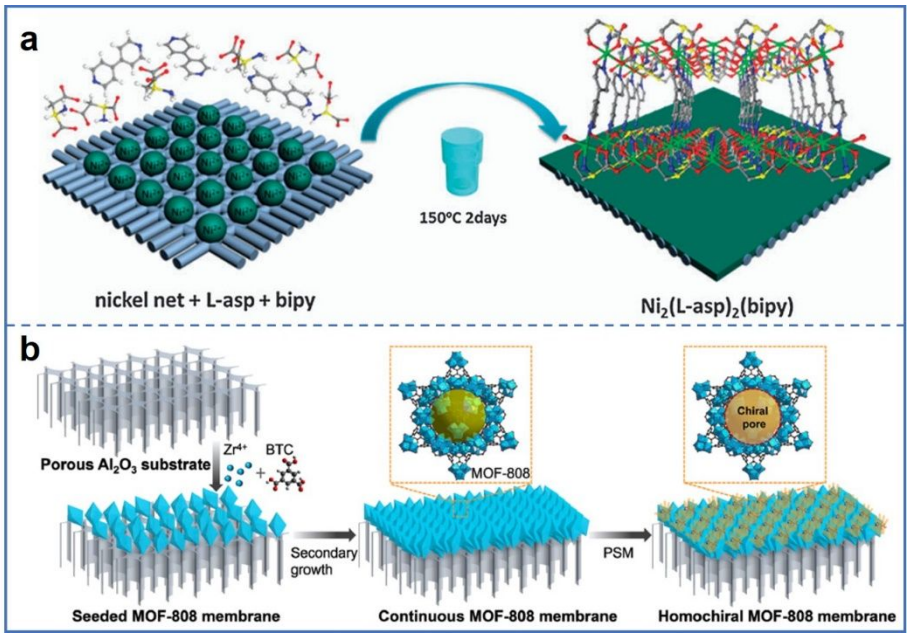

Fig. 2 (a) Ni net served as the substrate and metal source to coordinate with ligands under solvothermal conditions to form chiral Ni_2(*l*-asp)$_2$(bipy) membrane with thin thickness. Reproduced with permission from ref. 27. Copyright 2013 The Royal Society of Chemistry. (b) The achiral MOF-808 membranes were prepared on α-Al_2O_3 substrate using the secondary growth method, and then chiral molecules were introduced onto the metal clusters of MOFs through post-synthetic modification to obtain chiral MOF-808 membranes. Reproduced with permission from ref. 23. Copyright 2024 American Chemical Society.

Layer-by-layer synthesis. In this method, the chiral MOF materials are deposited onto the substrate layer by layer, which offers chiral MOF membranes with controllable thickness and low surface roughness. Heinke et al. prepared nanoporous chiral pillared-layer Cu_2(DCam)$_2$(AzoBiPyB) (DCam was *d*-camphoric acid, AzoBiPyB was (*E*)-2-(phenyldiazenyl)-1,4-bis(4-pyridyl)benzene)) membrane on the substrate using the controlled lbl method.[28] The pillar ligand AzoBiPyB in the chiral MOF provided photoswitchable property, while the interlayer ligand DCam provided chirality. Firstly, the substrate was immersed in metal salt solution for 15 min, then was washed with ethanol

and immersed in the mixed ligand solution for 30 min. After being washed with ethanol, the above process was repeated, and thin surface-mounted MOF membrane was grown layer by layer by alternately exposing the substrate to the precursor solutions. The thickness of MOF membrane could be regulated by changing the number of immersion cycles in the precursor solutions. The preparation of chiral MOF membrane on substrate in aqueous solution can be achieved through choosing the appropriate self-assembled monolayers (SAM) to modify the substrate. Gu et al. selected octathiolated γ-cyclodextrin ($\gamma CD(SH)_8$) as the SAM to modify Au substrate to prepare highly oriented surface-coordinated MOF (γCD-SURMOF) membrane (Fig. 3a).[29] The $\gamma CD(SH)_8$ with eight thiol groups reacted with Au to form thiolate bonds and was anchored on the Au surface, achieving surface functionalization of the Au substrate. Then, the modified Au substrate ($Au(\gamma CDS_8)$) was immersed in K ions and γCD aqueous solutions respectively, and the γCD-SURMOF was prepared by repeated lbl assembly. Unlike the chiral MOF membranes prepared from ethanol solution, the modified Au substrate did not require washing after each immersion. The thickness of γCD-SURMOF could be controlled by the number of cycles of immersion, and the membrane thickness increased as the number of cycles increased. Because $Au(\gamma CDS_8)$ induced direct nucleation, where the γCD ring was oriented parallel to the substrate in the presence of thiolate anchoring groups, the γCD-SURMOF exhibited the [110] orientation perpendicular to the substrate.

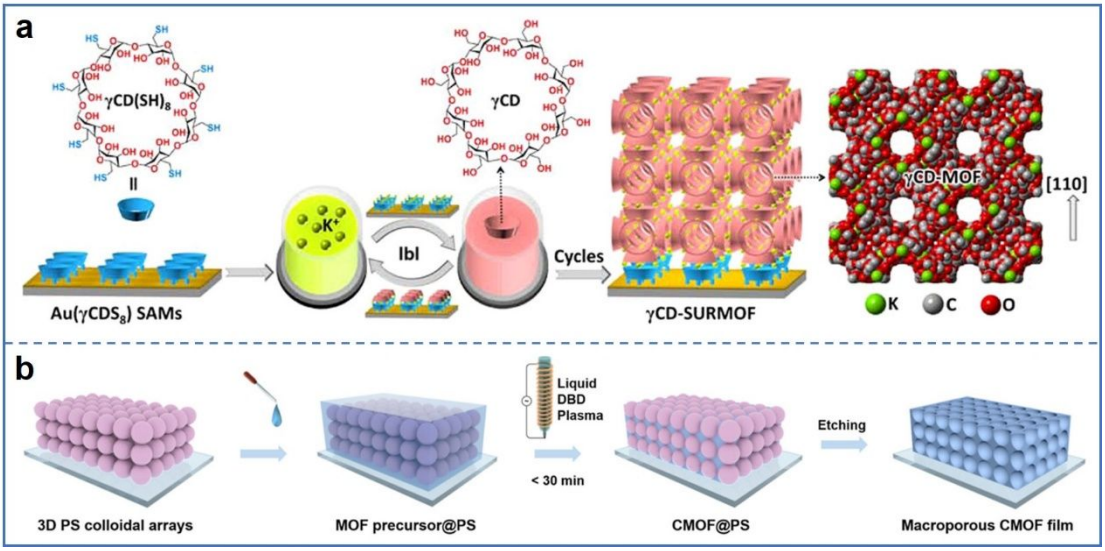

Fig. 3 (a) Metal ions and ligands were assembled layer by layer onto Au substrate modified with $\gamma CD(SH)_8$ through lbl synthesis to form γCD-SURMOF membrane. Reproduced with permission from ref. 29. Copyright 2022 Chinese Chemical Society. (b) M-CMOF membranes with hierarchical

View Article Online
DOI: 10.1039/D5NR00938C

porous structure were prepared by using PS arrays as templates for chiral MOF growth and then were removed using etching method. Reproduced with permission from ref. 30. Copyright 2024 American Chemical Society.

Template-assisted method. In this method, templates are used to provide extra pore structures for MOF membranes. Cui et al. recently reported the preparation of chiral His-ZIF-8, $[Cd(LTP)_2]_n$, and $[Cu(mal)bpy]\cdot H_2O$ membranes using template-assisted method, which not only possessed the inherent micropores in MOFs but also ordered macropores derived from template (Fig. 3b).[30] Polystyrene spheres (PSs) were assembled on glass slide to form highly ordered three-dimensional (3D) PS colloidal arrays, which were used as templates for MOF growth. Then, the PS arrays were immersed into the precursor solution of chiral MOFs and introduced into the liquid dielectric barrier discharge (DBD) plasma reactor. Three different chiral MOFs were grown in the interstices of PSs using DBD plasma induction method, and then the PSs template was removed by etching to obtain macro–microporous chiral MOF (M-CMOF) membranes with hierarchical porous structure of macropores and micropores. The preparation of chiral MOFs by liquid DBD plasma induced crystallization was a green synthesis approach with the advantages of short synthesis time, low cost, and low energy consumption. The three M-CMOF membranes exhibited good crystallization before and after template removal, with macropores in the membranes measuring approximately 200 nm. The M-*l*-His-ZIF-8 membrane exhibited an ultrathin thickness of ~3.9 μm. The presence of C=O stretch of chiral molecule *l*-His and the disappearance of N-H vibration indicated that the chiral molecule was incorporated into the MOF framework.

2.2. Chiral MOF MMMs

Chiral MOF MMMs are hybrid membranes in which chiral MOF fillers are embedded in the continuous matrix.[31] Chiral MOF MMMs are endowed the higher mechanical strength, less defect, and better continuity, due to combination of matrix. We will introduce the synthesis of chiral MOF materials and then the preparation of MMMs in the following.

2.2.1. Preparation of chiral MOFs

The quality of chiral MOFs materials will significantly affect the properties of chiral MOF MMMs. There are mainly three methods: in-situ synthesis, post-synthetic modification, and chiral induction, which suit for synthesis of various chiral MOFs (Fig. 4).[32,33]

View Article Online
DOI: 10.1039/D5NR00938C

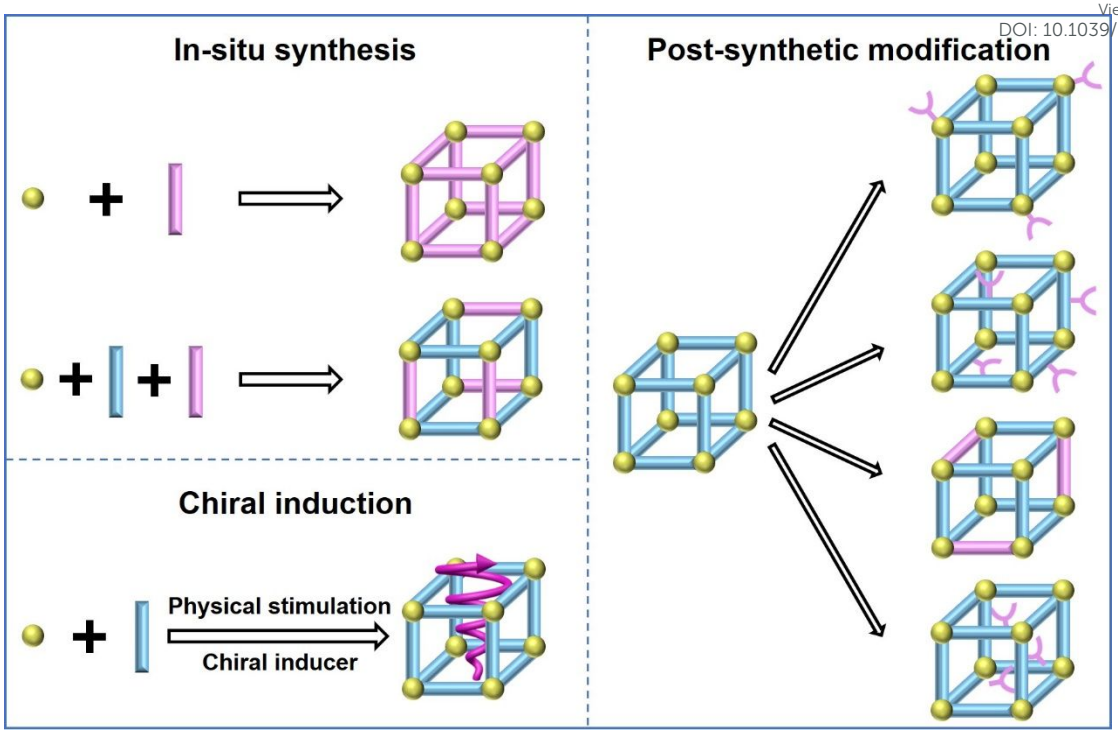

Fig. 4 The preparation methods of chiral MOFs include in-situ synthesis, post-synthetic modification, and chiral induction. Yellow balls represent metal nodes, blue sticks represent organic ligands, purple sticks represent chiral ligands, and purple Y-shaped curves represent chiral molecules.

In-situ synthesis. The in-situ synthesis is the most widely used method for synthesizing chiral MOFs, and the synthesized chiral MOFs exhibit bulk uniformity and high enantiomeric purity.[34-36] The method involves enantiomeric chiral ligands, which are expensive, causing complexity and high cost in the synthesis.

Tanaka et al. synthesized chiral ligands (R)-2,2'-dihydroxy-1,1'-binaphthyl-5,5'-dibenzoic acid (H_2L1) and (R)-2,2'-dimethoxy-1,1'-binaphthyl-5,5'-dibenzoic acid (H_2L2) for chiral interpenetrating (*R*)-MOF-1 and non-interpenetrating (*R*)-MOF-2, respectively (Fig. 5a).[37] In (*R*)-MOF-1, Cu ions coordinated with the four oxygen atoms in the carboxylic acid group of H_2L1 to form layers in the topological structure. Then, each two-dimensional (2D) network interpenetrated in the parallel or parallel tilted manner to form (*R*)-MOF-1. The 2D network structure in (*R*)-MOF-2 was like that in (*R*)-MOF-1, but the 2D network did not interpenetrate but overlapped to form (*R*)-MOF-2. In addition, Wang et al. synthesized the homochiral *l*-His-ZIF-8 through using mixed ligands.[19] The chiral molecule *l*-histidine (*l*-His) was introduced into the precursor solution of ZIF-

View Article Online
DOI: 10.1039/D5NR00938C

8, and then *l*-His-ZIF-8 was formed by solvothermal self-assembly of *l*-His with 2-methylimidazole (Hmim) and Zn ions.

The in-situ synthesis method has also been used in the synthesis of chiral MOF nanosheets with highly ordered in-plane nanopores, which exhibit excellent performance in catalysis, sensing, and separation. For example, Cui et al. synthesized chiral layered Eu-MOF using dicarboxylic acids derived from 1,1'-biphenyl phosphoric acid as chiral ligands.[38] Eu ions were coordinated with four bidentate bridges and four chelating carboxylate groups in six ligands. Two adjacent Eu ions were connected by four carboxylate groups to form a planar framework, which was then stacked vertically to form the layered structure. The layered Eu-MOF was exfoliated into chiral MOF nanosheets (1-MONs) by using solvent assisted liquid sonication due to weak interlayer interactions between layers.

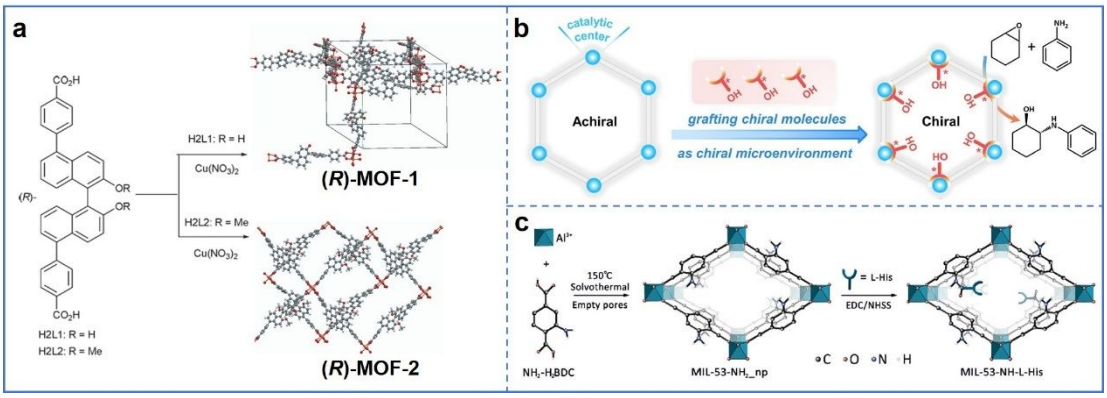

Fig. 5 (a) Chiral molecules H_2L1 and H_2L2 were used as ligands to prepare chiral (*R*)-MOF-1 and (*R*)-MOF-2 through in-situ synthesis. Reproduced with permission from ref. 37. Copyright 2015 The Royal Society of Chemistry. (b) Chiral (*R*)-C_n@PCN-222(Cu) was prepared by anchoring chiral molecules onto unsaturated coordinated Zr clusters in PCN-222(Cu). Reproduced with permission from ref. 43. Copyright 2023, Wiley-VCH. (c) Chiral MIL-53-NH-*l*-His was prepared by grafting *l*-His onto ligands of the as-synthesized MIL-53-NH_2(Al) due to the amidation reaction between *l*-His and ligands. Reproduced with permission from ref. 44. Copyright 2019, Wiley-VCH.

Post-synthetic modification. This method involves introducing chiral molecules into the as-synthesized achiral MOFs to endow them with chiral characteristics without altering their topological structure.[39-42] When there are active sites in MOFs, chiral molecules can be grafted onto the metal clusters or organic ligands of MOFs through coordination or covalent interactions. This

View Article Online
DOI: 10.1039/D5NR00938C

method is successfully applied for a wide variety of chiral MOFs, as it starts from achiral materials, with the chirality introduced in a separate process. However, compatibility and interaction with MOFs needs to consider during the selection of chiral molecules.

PCN-222(Cu) is an achiral MOF formed by the coordination of Zr ions, [5,10,15,20-Tetrakis(4-carboxyphenyl) porphyrinato]-Cu(II) (Cu-TCPP), and benzoic acid (Fig. 5b).[43] By anchoring chiral hydroxylated molecules with different carbon chain lengths onto unsaturated coordination sites of Zr clusters, a series of (*R*)-C_n@PCN-222(Cu) (n = 1, 2, 3) were obtained. There were approximately 3.8-3.9 chiral molecules grafted onto each Zr cluster on average, indicating that chiral molecules completely replaced the -OH groups on Zr clusters and coordinated with Zr clusters.

Wang et al. introduced the chiral molecule *l*-His that can coordinate with the functional groups of ligands to convert achiral MIL-53-NH_2(Al) into chiral MIL-53-NH-*l*-His (Fig. 5c).[44] The achiral MIL-53-NH_2(Al) was formed by the coordination assembly of Al clusters with 2-aminoterephthalic acid (NH_2BDC) with flexible framework structure, which was conducive to immobilizing guest molecules. The carboxylic group in *l*-His underwent amidation reaction with the amino group in NH_2BDC to graft *l*-His into the MOF framework, endowing MIL-53-NH_2(Al) with chirality.

In addition to grafting chiral molecules onto ligands, chiral MOFs can also be achieved by replacing achiral ligands in MOFs. Cui et al. used a solvent assisted ligand exchange strategy to incorporate chiral ligand linear dicarboxylate linkers (H_2L^M) into UiO-68-Me.[45] The H_2L^M molecule had similar length and connectivity with the ligand (2-methyl-terphenyl dicarboxylate ligand) H_2TPDC-Me in UiO-68-Me.

Incorporating chiral guests into the pores of MOFs is also a post-synthetic modification method. The chiral molecules [Rh(Me-BPE)(cod)]OTf were encapsulated into the pores of UMCM-1-NH_2, endowing the MOF with chiral properties, which exhibited excellent enantioselectivity in asymmetric hydrogenation reactions of unsaturated olefins.[46] During the post-synthetic modification process, it is necessary to strictly control the reaction conditions to avoid damaging the MOF framework structure.

Chiral induction. Chiral induction is based on achiral precursors, where the symmetry breaking and induction of chiral arrangement in building units are caused by physical stimulation such as CPL irradiation, or adding inducing agents.[47-49] Chiral induction method is relatively simpler and less expensive but giving less pure products.

View Article Online
DOI: 10.1039/D5NR00938C

Wu et al. synthesized the coordination polymer [{*P*/*M*-Cu(succinate)(4,4'-bipyridine)}$_n$]·(4 H_2O)$_n$ using CPL irradiation.[50] According to the analysis of CPL chirality and corresponding obtained products, the product after left-handed CPL irradiation showed a left-handed helical structure, while right-handed CPL irradiation was beneficial for the production of right-handed helical structure crystals. The Cu ions coordinated with succinic acid to form an intermediate fragment [Cu(succinate)]$_x$, which exhibited helicity. CPL irradiation stimulated the conversion of fragment [Cu(succinate)]$_x$ into the preferential configuration, which then assembled into a 3D structure with chirality by coordinating with 4,4'-bipyridine.

In addition to physical stimulation, introducing chemical reagents can also induce the chirality by affecting the self-assembly of MOFs. Enantiomeric pure organic acids D-(+)-camphoric acid (D-(+)-H_2cam) and L-(−)-camphoric acid (L-(−)-H_2cam) were used to induce asymmetric crystallization of achiral manganese damantane-1,3-dicarboxylic ([Mn(adc)]) (Fig. 6a).[51] When using D-(+)-H_2cam as a chiral inducer, the main product was (+)-[Mn_3(HCOO)$_4$(adc)]; When L-(−)-H_2cam was used as a chiral inducer, the main product was (−)-[Mn_3(HCOO)$_4$(adc)]. The synergistic effect of chiral H_2cam and achiral H_2adc led to asymmetric crystallization of the product. H_2cam coordinated with Mn clusters to control the absolute helicity of the [Mn_3(HCOO)$_4$]$_n^{2n+}$ framework. Then, the H_2cam in the crystal was replaced by H_2adc ligands to form chiral MOFs, and H_2cam was not incorporated into the MOF structure. Hong et al. introduced chiral intermediates I(*M*) or I(*P*) to the assembly with achiral pyridine, ligand benzene-1,3,5-tris(4-benzoic acid) (H_3BTB) and Zn ions, to prepare chiral FJI-H27(*M*) and FJI-H27(*P*) (Fig. 6b).[52] Pyridine, as a template, participated in the coordination driven assembly, the amount of which provided the precise regulation of the chirality.

In conclusion, the in-situ synthesis offers high enantiomer purity and stability, even though it is complex and expensive, usually requiring the high temperature and pressure. Post-synthetic modification is a general method, in which the compatibility of the introduced chiral molecules and MOFs needed to be required. The chiral induction method is simple and cost-effective, even though chiral purity achieved is modest. Depending on the requirements on chiral MOFs, various preparation methods are available.

View Article Online
DOI: 10.1039/D5NR00938C

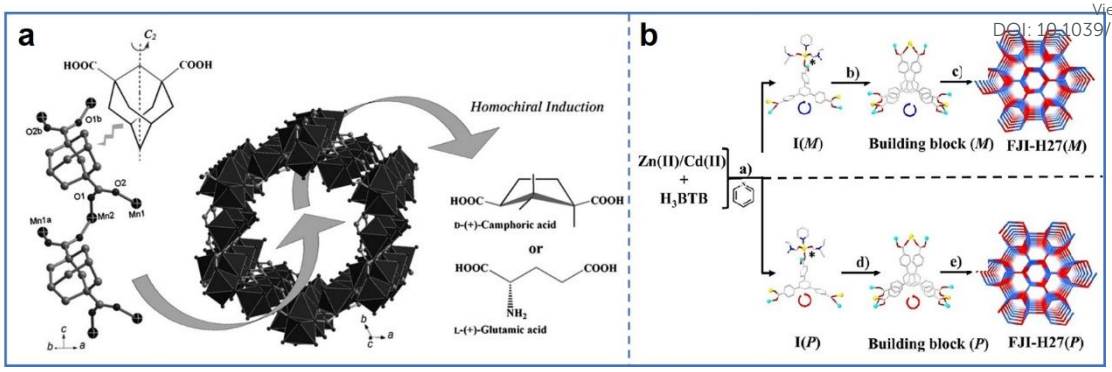

Fig. 6 (a) H_2cam, as the chiral inducer, participated in the coordination of MOFs, firstly coordinating with Mn clusters and then being replaced by ligands, endowing the product $[Mn_3(HCOO)_4(adc)]$ with chiral properties. Reproduced with permission from ref. 51. Copyright 2010, Wiley-VCH. (b) The achiral pyridine acted as chiral inducer to participate in the coordination of MOFs to form chiral intermediates, which were then substituted by ligands to form chiral FJI-H27(*M*) and FJI-H27(*P*). Reproduced with permission from ref. 52. Copyright 2021, Wiley-VCH.

2.2.2. Preparation of chiral MOF MMMs

Chiral MOF MMMs are prepared by dispersing chiral MOF particles in a matrix and using specific molding processes to obtain membranes with chiral properties. The key to this preparation approach is the uniform dispersion and good interfacial compatibility of MOF particles with the matrix. Polymers are widely used as the matrix for chiral MOF MMMs, as the polymers are soft and provide functional groups to interact with the ligands of MOFs. The preparation methods of chiral MOF MMMs include solution casting and TIPS-HoP.

Solution casting. The solution casting method involves mixing chiral MOFs with polymers and casting them into a membrane, followed by appropriate post-treatment to obtain the final MMMs, which is simple and suitable for large-scale production. Wang et al. prepared MIL-53-NH-*l*-His based MMM by depositing the membrane onto substrate using a casting blade to apply solution or paste (Fig. 7a).[44] Firstly, a small amount of polymer polyethersulfone (PES) was added to chiral MOF particle dispersion to reduce the aggregation of MOF particles in the polymer. Then, the remaining PES was added to the dispersion and stirred evenly. Subsequently, the mixture was dropped onto a glass substrate and spread into a membrane on the substrate using a casting blade. As the solvent evaporated, MIL-53-NH-*l*-His based MMM was formed, which could be peeled off from the glass substrate after cooling to obtain self-supporting membrane. MIL-53-NH-*l*-His

View Article Online
DOI: 10.1039/D5NR00938C

particles were uniformly distributed in the membrane without cracks and defects (Fig. 7b). The loading of MOFs in the membrane could be regulated by changing the ratio of added MOFs. MMMs with different loading ratio of MOFs retained the crystal structure of MOF particles, indicating that the manufacturing process of the membrane did not affect the crystal structure of MOFs.

Later, the group used the same preparation method to mix chiral MOF γ-CD-MOF with PES to prepare CD-MOF/PES MMMs.[53] In addition to PES as the polymer substrate, poly(vinylidene fluoride) (PVDF) was also employed as the dispersed matrix for yolk-shell *l*-His&R6G@ZIF-8 particles in the preparation of MMMs.[54] The casting blade technology is simple and effective for preparing MMMs with controlled thickness and surface roughness.

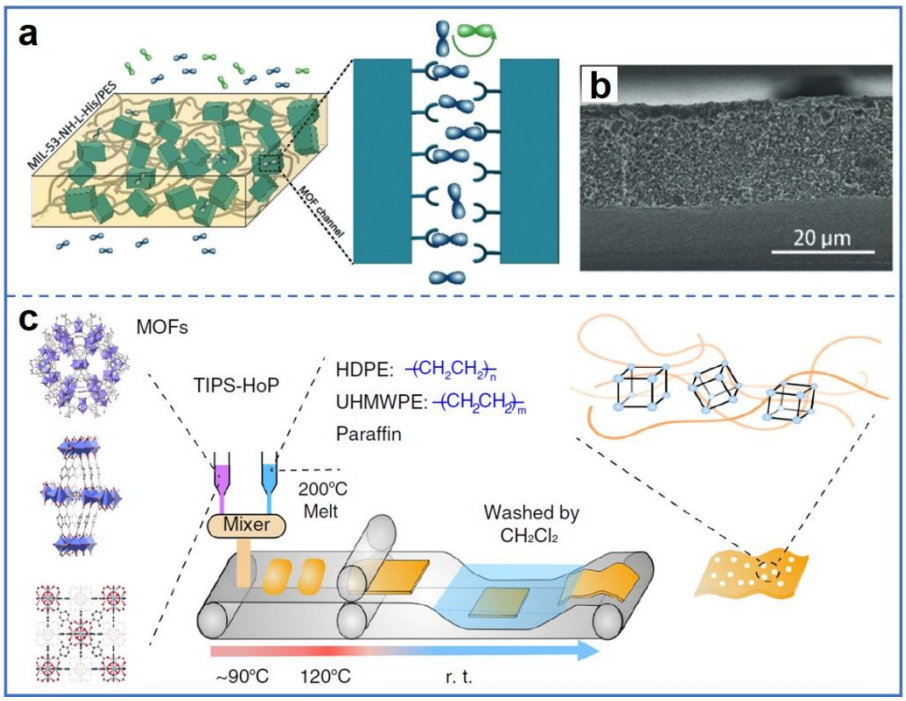

Fig. 7 (a) Chiral MIL-53-NH-*l*-His was uniformly dispersed in PES to prepare self-supporting MMMs by solution casting method. (b) SEM image of the cross-section of MMMs with 20 wt% MIL-53-NH-*l*-His loading. Reproduced with permission from ref. 44. Copyright 2019, Wiley-VCH. (c) Chiral Zn-BLD was dispersed into mixed polymers HDPE and UHMWPE to prepare MMMs with high MOF loading through TIPS-HoP method. Reproduced with permission from ref. 55. Copyright 2019, Springer Nature.

TIPS-HoP. This method involves roll-to-roll hot pressing the mixture of ultra-high molecular weight polymer interwoven MOF particles onto a belt to form MMMs, which usually help achieve

View Article Online
DOI: 10.1039/D5NR00938C

membranes with good flexibility and ultrahigh MOF loading. MOFs act as the molecular sieving channel in MMMs, in which the separation performance can be effectively improved through increasing the loading of MOFs.

Wang et al. prepared the MMMs using the TIPS-HoP approach, which overcame the challenge of loss of mechanical strength in high MOF-loading membranes (Fig. 7c).[55] Firstly, chiral Zn-BLD was added to the paraffin, high-density polyethylene (HDPE), and ultrahigh-molecular-weight polyethylene (UHMWPE) mixed melt, and continuously stirred to disperse evenly. UHMWPE was introduced into the membrane to connect MOF particles, ensuring the flexibility of the membrane under ultrahigh MOF loading. Paraffin was used as the flowable agent to reduce the melt viscosity of HDPE and UHMWPE, avoiding the formation of membranes with brittleness and impermeability. Then, the mixture was dropped onto a belt and transferred to the middle of two rollers for roll to roll hot pressing to form the MMM. Finally, Zn-BLD PE MMM was formed by soaking the membrane in dichloromethane to remove paraffin in the membrane. In addition to chiral Zn-BLD, achiral MOFs such as NH_2-UiO-66, MIL-100(Cr), MOF-5, and ZIF-8 could be prepared as MMMs using this approach, demonstrating the universality of this strategy. Usually, the mechanical properties of MMMs decreased with the increasing of MOF loading.[56,57] However, the MMM with 86% MOF (Zn-BLD PE MMM-86%) loading kept the flexibility without forming cracks after bending. MOF particle aggregates and long-chain polymers interwove in Zn-BLD PE MMM-86%, forming hierarchical porous structured MMM with the inherent micropores of MOFs and the macropores originated from the interweaving of MOF particles.

Recently, some reports investigated some new matrices for chiral MOF MMMs. Chiral liquid crystal (CLC) was introduced to combine with MOFs to prepare CLC MOF (CLCMOF) membrane. Gu et al. prepared CLCMOF membrane by combining CLC with $Zn_2(sdc)_2$ (Fig. 8a).[58] The CLC solution was a mixture of R-obob, 2-methyl-1,4-phenylene bis(4-(3-(acryloyloxy)propoxy)benzoate) (MPBAB), and 4-[[6-[(1-oxo-2-propen-1-yl)oxy]hexyl]oxy]-,4-methoxyphenyl ester (OHOMP) in a certain proportion, which encapsulated into the pores of $Zn_2(sdc)_2$, due to cross-linking reaction between alkenyl groups in CLC and stilbene groups in MOF ligands under ultraviolet light (UV) irradiation. The CLCMOF membrane exhibited LC thermotropic property and excellent transparency. The crystal structure of $Zn_2(sdc)_2$ was not destroyed after cross-linking reaction with CLC, allowing the CLCMOF membrane to retain the crystallinity of MOFs.

View Article Online
DOI: 10.1039/D5NR00938C

Xu et al. used an amorphous metal-polyphenol network (MPN) as the matrix for an amorphous/crystalline heterogeneous structure chiral MOF membrane (MPN-DMOF) (Fig. 8b).[59] MPN was prepared by the mixed solution of Cu^{2+}, polyethylenimine (PEI), and tannic acid (TA), and provided abundant nucleation sites, where the D-methionine chelated with Cu ions to form MOFs. The MPN-DMOF coating retained the crystal structure and phase purity of D-Met@MOF constructed by Cu clusters with D-methionine ligands.

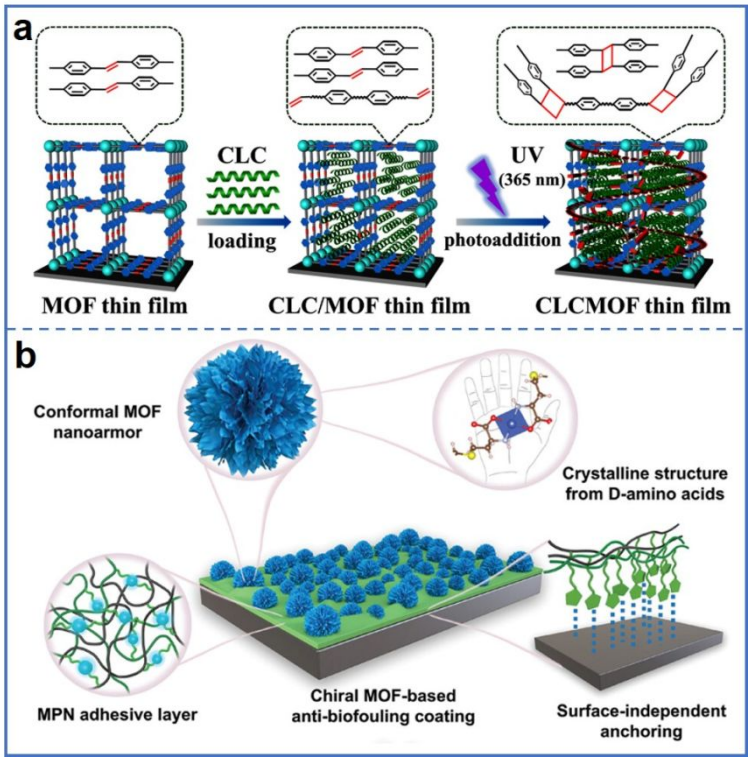

Fig. 8 (a) CLC was encapsulated into the pores of achiral MOFs using lbl method, and then crosslinked with MOFs through photocycloaddition reaction under UV irradiation to obtain CLCMOF membrane. Reproduced with permission from ref. 58. Copyright 2024 American Chemical Society. (b) Chiral molecules acted as ligands to mineralize on MPN substrate and self-assembled with Cu ions in the substrate to form chiral MOFs, leading to the formation of MPN-DMOF coatings. Reproduced with permission from ref. 59. Copyright 2024, Wiley-VCH.

To conclude, pure chiral MOF membranes provide high porosity and more accessible active sites, even though the high cost, and lack of self-supporting possibility. Chiral MOF MMMs have excellent mechanical strength and more convenient applications as self-supporting membranes. However, the interface compatibility between MOFs and matrices, as well as the aggregation of

View Article Online
DOI: 10.1039/D5NR00938C

MOF particles, are still to be improved for high-quality MMMs.

3. Applications of chiral MOF membranes

High porosity and high density of reactive sites ensure the chiral MOF membranes great potentials for chiral recognition and enantiomer separation.[60-62] By involvement of luminescent units in various ways, chiral MOF membranes also present the excellent CPL properties, which make them potential for applications in optical display and information storage fields.[63] We discussed the applications of chiral MOF membranes in sensing, separation, and CPL in the following.

3.1. Sensing

Due to the abundant active sites and decoration of chiral units, chiral MOF membranes interact differently with chiral enantiomers, and have been successfully applied as sensors to distinguish chiral isomers.[64-67]

Cui et al. dispersed chiral 1-MONs into PES to prepare self-supporting MMM (1-MONs-MMM) for detecting terpenes and terpenoids, which was a challenging enantiomer detection issue.[38] 1-MONs-MMM exhibited the emission peak at 355 nm, which was blue shifted compared to 386 nm of 1-MONs in acetonitrile solvent. This might be due to the influence of PES matrix in the MMM on fluorescence emission. The phosphoric acid active sites in 1-MONs interacted with the double bonds or carbonyl groups in terpenes and terpenoids, which induced changes in the structure of the nanosheets, such as conformational and exciton binding changes or hardening, leading to fluorescence quenching and selective recognition of enantiomers (Fig. 9a). When MMMs were exposed to (−)-linalool vapor, the fluorescence of (*S*)-1-MONs-MMM and (*R*)-1-MONs-MMM was quenched (Fig. 9b). After 420 s, the quenching percentage of (*S*)-1-MONs-MMM reached 38.5%, while the quenching percentage of (*R*)-1-MONs-MMM could only reach to 6.5%, corresponding to the enantioselectivity factor of 9.03 (Fig. 9c). MMMs selectively recognized not only chiral vapors with single functional groups such as α-pinene, limonene, and fenchone, but also terpenoids with chiral bifunctional groups including terpinen-4-ol and β-citronellol. In addition to chiral MOF nanosheets, L-His&R6G@ZIF-8 with the unique yolk-shell structure MMMs have also been prepared as optical sensors for highly sensitive and selective detection of L-proline.[54]

View Article Online
DOI: 10.1039/D5NR00938C

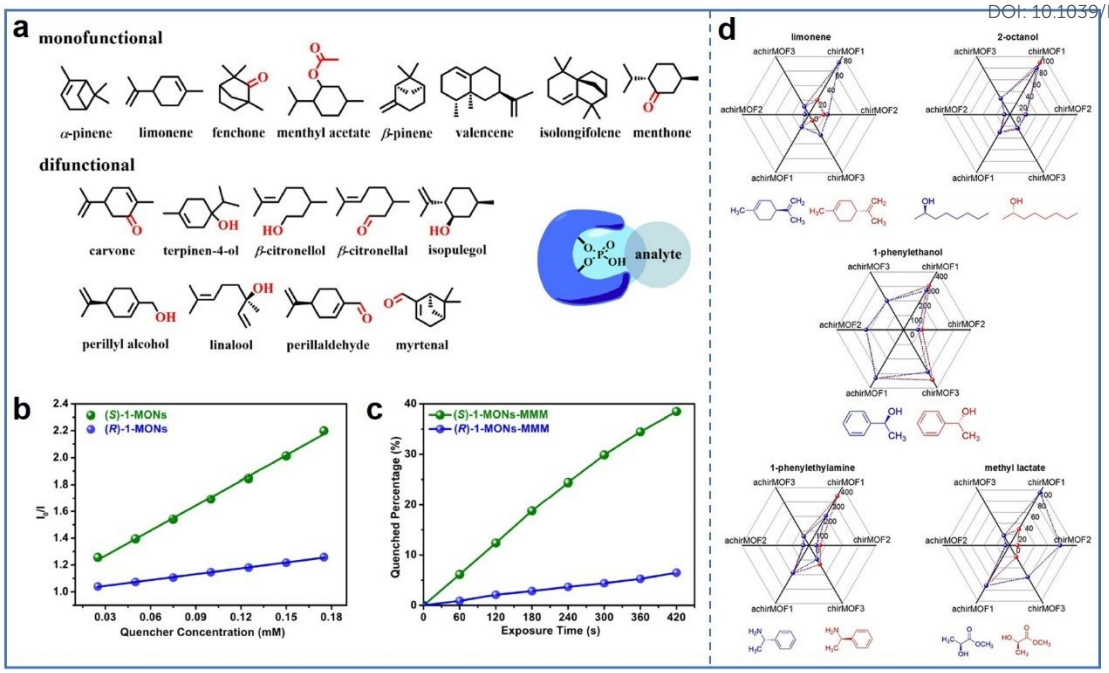

Fig. 9 (a) The structures of monofunctional and difunctional terpenes and terpenoids. The detection principle of the sensor was that the interaction between the phosphoric acid active sites in 1-MONs and the double bonds or carbonyl groups in terpenes and terpenoids quenched the fluorescence. (b) Stern–Völmer plots of (−)-linalool added to 1-MONs. (c) The quenching percentage of (*S*)-1-MONs-MMM and (*R*)-1-MONs-MMM when (−)-linalool exposed to the membranes. Reproduced with permission from ref. 38. Copyright 2021 American Chemical Society. (d) Radar plots response of sensors exposed to five enantiomers. Reproduced with permission from ref. 69. Copyright 2021, Wiley-VCH.

In order to simultaneously identify multiple molecules and their enantiomers, the sensor array composed of different sensors for identifying enantiomers has been proposed.[68] Heinke et al. prepared the enantioselective electronic nose (e-nose) based on chiral MOF sensor array and used for the detection of chiral odor molecules through machine learning.[69] Three chiral MOFs and three achiral MOFs were prepared as quartz-crystal microbalance (QCM) sensors, which were integrated into the sensor array. In the e-nose, achiral MOFs were only used to distinguish different molecules, exhibiting the same response as chiral isomers, while chiral MOFs were used to recognize enantiomers. When the sensor array was exposed to odor molecules, the contact between MOF membranes and odor molecules caused a frequency shift in resonance frequency to achieve response

View Article Online
DOI: 10.1039/D5NR00938C

to odor molecules, and the sensor response was linearly correlated with the concentration of odor molecules. The sensor array exhibited selective recognition of ten isomers with an average accuracy of 96.1%, achieving high selectivity recognition (Fig. 9d).

Later, the same group used MOF membrane sensor arrays to detect mixtures of ternary xylene isomers.[70] The accuracy of e-nose to distinguish isomers of xylene mixtures with concentrations of 10 ppm and 100 ppm was tested. By using machine learning algorithms to analyze sensor array data, the composition of the mixture could be determined. The accuracy of the mixture with 10 ppm concentration was 86%, and the accuracy of the mixture with 100 ppm concentration could reach to 96%. When the concentration of the mixture was 100 ppm, the sensor array could recognize sixteen different xylene mixtures.

Recently, Gu et al. prepared ZnCar SURMOFs membranes with dynamic structural changes for selective recognition of six fragrance enantiomers ((+)/(−)-carvone, (+)/(−)-menthol, and (+)/(−)-limonene), mimicking the conformational changes of olfactory receptor proteins.[71] ZnCar SURMOFs were prepared by ligands of L-carnosine (Car) and Zn ions with the lbl method. A chiral sensor was constructed by integrating ZnCar SURMOFs into a QCM, showing a high recognition accuracy (98.58%) for fragrance enantiomers.

Electrochemical devices are widely applied in chiral sensing due to their advantages of high sensitivity, high selectivity, low cost, and good stability.[72,73] Chiral MOF can be deposited onto electrodes for electrochemical chiral recognition.[74] For example, Zheng et al. immobilized chiral MOF nanofibers in chitosan (CS) to prepare the MOF/CS electrochemical sensor for selective detection of tyrosine (Tyr) enantiomers.[75] MOF and MOF/CS modified glassy carbon electrodes (GCE) exhibited higher interfacial charge transfer resistance compared to CS modified GCE, indicating that the introduction of CS improved electron transfer. Due to the synergistic effect of chiral MOF nanofibers and chiral CS, MOF/CS displayed the maximum peak current ratio, which was more sensitive for the detection of Tyr enantiomers. The concentrations of D/L-Tyr in the range of 0.007-0.055 mM were linearly correlated with peak current of D/L-Tyr oxidation, demonstrating the quantitative detection of Tyr isomers. Compared with the initial current, the current loss after ten days was only 8.9%, indicating that the MOF/CS electrochemical sensor exhibited good repeatability and stability.

The chiral environment, such as nanoconfined spaces, has a significant impact on chiral

recognition. Xia et al. revealed the influence of chiral environment on chiral recognition by comparing the detection of three amino acids of enantiomers (tryptophan (Trp), Alanine (Ala), and leucine (Leu)) with different sizes.[76] The dense chiral c-ZIF-8 layer was deposited on a gold coated poly(ethylene terephtalate) (PET) nanochannel array using cathodic deposition method, forming the c-ZIF-8-PET chiral membrane for electrochemical recognition. The selectivity is only found in enantiomers of Trp, among three amino acids, as the chiral cavity size of c-ZIF-8 (8.1 Å) matched the molecular size of Trp but not Ala and Leu (Fig. 10a). After adding L-Trp, the zeta potential of c-ZIF-8 increased, while the zeta potential remained almost unchanged after adding D-Trp (Fig. 10b). This is attributed to the selective adsorption of negatively charged L-Trp molecules by the c-ZIF-8 layer, which increased the surface charge density and led to an increase in zeta potential. The continuous expansion of the D-Trp downward peak at 234 nm further indicated the sustained adsorption of L-Trp by c-ZIF-8 (Fig. 10c). The imidazole ring in D-Trp exhibited steric hindrance effect, making it difficult to enter the chiral cavity of c-ZIF-8. The high adsorption capacity of c-ZIF-8 layer for L-Trp was beneficial for the interaction between L-Trp and chiral sites, thereby facilitating chiral recognition. The work indicated the important role of size matching effect in chiral recognition.

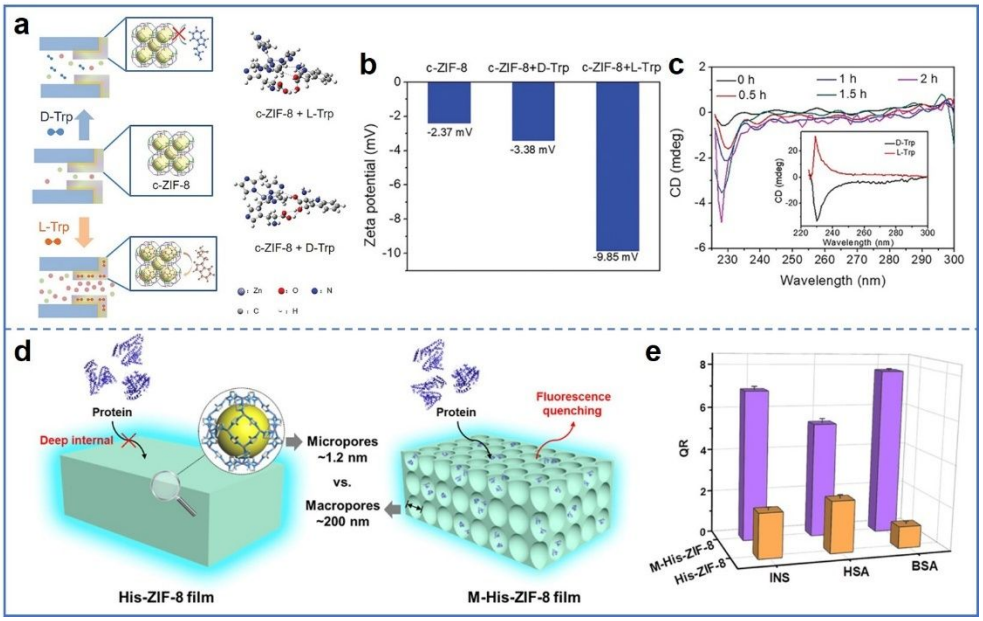

Fig. 10 (a) Schematic diagram of the interaction and adsorption differences between D-Trp, L-Trp, and c-ZIF-8. (b) The zeta potential of c-ZIF-8 membrane and c-ZIF-8 membrane with added D-Trp or L-Trp. (c) CD spectra of c-ZIF-8 interacting with Trp racemic mixture at different times. Reproduced with permission from ref. 76. Copyright 2023, Wiley-VCH. (d) Proteins could not enter

View Article Online
DOI: 10.1039/D5NR00938C

the *l*-His-ZIF-8 membrane but could enter and interact with M-*l*-His-ZIF-8 membrane to quench the fluorescence. (e) The quenching ratio values of INS, HSA, and BSA in contact with M-His-ZIF-8 membrane and His-ZIF-8 membrane. Reproduced with permission from ref. 30. Copyright 2024 American Chemical Society.

The chiral MOF membranes usually have microporous structures, where biomolecules can hardly enter, making the recognition of biomolecules challenging. To overcome this challenge, Cui et al. prepared chiral MOF M-*l*-His-ZIF-8 membrane with hierarchical pores for detecting both the small molecules and large proteins.[30] Chiral MOF M-*l*-His-ZIF-8 membrane provides highly selective detection of phenylethanol enantiomers. In detail, fluorescence intensity of the membrane was significantly enhanced by (*R*)-phenylethanol, but did not change with (*S*)-phenylethanol. The *l*-His part in MOF interacted with the hydroxyl group in phenylethanol through hydrogen bonding, and the interaction between *l*-His-ZIF-8 and (*R*)-phenylethanol was stronger compared with (*S*)-phenylethanol.

Furthermore, M-CMOF membrane with macropores and micropores structures exhibited excellent chiral recognition for proteins such as human serum albumin (HSA), bovine serum albumin (BSA), and insulin (INS) with high enantioselectivity (Fig. 10d and e). The M-*l*-His-ZIF-8 membrane still retained the integrity of the macropores structure after 3 months and could be reused at least 5 times, indicating the excellent stability and recyclability of the membrane.

Wearable smart biosensors for human health monitoring were also prepared by chiral MOF membranes. Xie et al. constructed flexible MMMs with RT@CDMOF and PES for wearable sensors to detect lactic acid in sweat and monitor fatigue levels in high-intensity exercise.[25] In RT@CDMOF, the dual response was achieved by encapsulation of both rhodamine 6G hydrazide (RGH) with fluorescence response and tetracyanovinylindane (TCN) with colorimetric response in γ-CDMOF. With the distinguishable color change and different affinity of L-lactic and D-lactic to MOF materials, RT@CDMOF MMMs exhibited rapid dual color sensing of lactic acid enantiomers with biocompatibility, flexibility, and mechanical stability, which was beneficial for health monitoring.

Chiral MOF membranes have been used for the recognition of various chemical enantiomers. The selective sensitivity was achieved by the different interactions between target molecules and chiral

View Article Online
DOI: 10.1039/D5NR00938C

sites or structures. The various signal outputs, such as fluorescence or colorimetry, provide diversity visual view. However, some improvements are still needed in chiral MOF membranes, e.g., recognition ability of target molecules in complex matrices, stability of chiral MOF membranes in specific chemical or physical environments.

3.2. Separation

To avoid ineffective or even harmful effect from enantiomer of a designed chiral material in drug or food additives, it is significant separate the enantiomers for pure designed single configuration.[77,78] By design on pore structure and surface chemistry, chiral MOF membranes have also been successfully applied for chiral enantiomer separation.[79,80]

Chiral alcohols are important precursors for the synthesis of chiral drugs.[81] Among them, the 1-phenylethanol is widely used, to be specific, *S*-1-phenylethanol is used for drugs to treat depression and asthma, while *R*-1-phenylethanol is a useful ophthalmic preservative and cholesterol adsorption inhibitor. Therefore, the separation of chiral enantiomers in 1-phenylethanol is of great significance. Wang et al. prepared *l*-His-ZIF-8 membrane for the separation of racemic 1-phenylethanol (Fig. 11a).[19] *l*-His introduced the chiral environment into the MOF channel, thereby endowing MOF with enantioselectivity. The peak shift of the membrane after permeation with 1-phenylethanol at 14 ppm and 124 ppm in solid-state nuclear magnetic resonance (NMR) indicated that the interaction between chiral molecules and MOF was very close at the molecular level to the two sites in space (Fig. 11b). Due to the difference of interaction *S*-1-phenylethanol and with *R*-1-phenylethanol *l*-His-ZIF-8, they permeate through the membrane at a difference rate, fulfilling the enantiomeric separation with excess value (*ee*) with 76% (Fig. 11c). The membrane could separate enantiomers three times without losing selectivity, and the crystal structure of *l*-His-ZIF-8 remained unchanged. To further improve the separation performance, they used chiral MIL-53-NH-*l*-His MMMs for the separation of 1-phenylethanol racemization with 100% *ee*.[44]

The same group also prepared CD-MOF/PES MMMs for the separation of racemic 1-phenylethanol with 100% *ee* (Fig. 11d).[53] In this work, the influence of solvent polarity on separation performance was studied. The increase of solvent polarity led to a decrease in the enantioselectivity of the membrane, as polar solvents preferentially occupied chiral sites in MOFs, leading to reduced adsorption of 1-phenylethanol in MOFs (Fig. 11e). In addition, assembling chiral MOF membranes into capillary column was also used for the separation of racemic 1-phenylethanol.

The chiral pillar-layered Cu_2(*d*-cam)$_2$P (*d*-cam was (1*R*,3*S*)-(+)-camphorate, P was 1,4-diazobicyclo[2.2.2] octane (dabco) and bipy) was grown layer by layer in a capillary column to form the membrane, which exhibited excellent separation efficiency for 1-phenylethanol.[82]

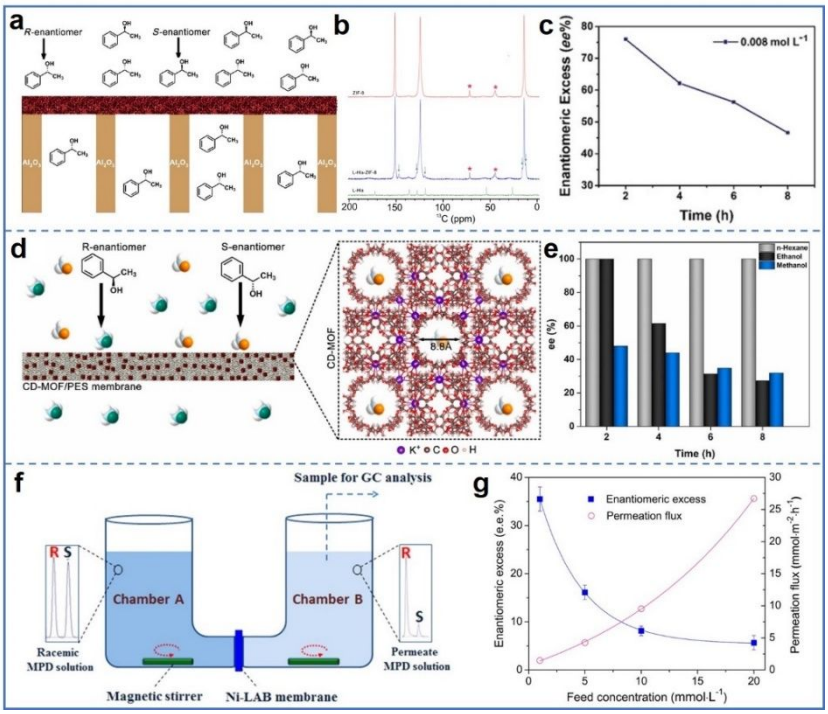

Fig. 11 (a) Schematic diagram of *l*-His-ZIF-8 membrane for separating racemic 1-phenylethanol. (b) ^{13}C CPMAS NMR spectra of ZIF-8, *l*-His-ZIF-8, and *l*-His. (c) The *ee*% as a function of time under the condition of 0.008 mol L^{-1} racemic 1-phenylethanol. Reproduced with permission from ref. 19. Copyright 2018, Wiley-VCH. (d) Schematic diagram of CD-MOF/PES MMMs separation of 1-phenylethanol racemic mixture. (e) The *ee*% values of 1-phenylethanol racemates dissolved in solvents with different polarity separated by MMMs. Reproduced with permission from ref. 53. Copyright 2021, Elsevier B.V. (f) Schematic diagram of separating racemic mixture of MPD at low temperature through Ni_2(*l*-asp)$_2$(bipy) membrane. (g) The *ee*% and permeation flux of Ni_2(*l*-asp)$_2$(bipy) membrane with different feed concentrations at 30 °C. Reproduced with permission from ref. 83. Copyright 2013, Wiley-VCH.

In addition to racemic 1-phenylethanol, 2-methyl-2,4-pentanediol (MPD), a type of dihydric alcohol, is an important intermediate in synthesis of fine chemicals and chiral drugs. Qiu et al. prepared chiral Ni_2(*l*-asp)$_2$(bipy) membrane on nickel net by in-situ growth method for the separation of MPD isomer mixtures.[27] Due to the interaction between *S*-MPD and chiral channels

View Article Online
DOI: 10.1039/D5NR00938C

in MOFs, (*S*)-MPD was adsorbed on the active sites, while (*R*)-MPD had a higher permeability. The chiral Ni_2(*l*-asp)$_2$(bipy) membrane also exhibited excellent thermal stability in addition to the effect for separation. Raising the separation temperature of the membrane from room temperature to 200 °C resulted in a higher permeability of *R*-MPD, leading to an *ee* value of 32.5% for racemic separation.

In the same year, Jin et al. reported the separation of MPD racemization at low temperatures using Ni_2(*l*-asp)$_2$(bipy) membrane (Fig. 11f).[83] Unlike the preparation method reported by Qiu et al., they decreased the crystal size of the as-synthesized Ni_2(*l*-asp)$_2$(bipy) crystals by ball milling and then followed by secondary growth to form the membrane. *R*-MPD was more easily passed through Ni_2(*l*-asp)$_2$(bipy) membrane with a higher permeability than *S*-MPD, achieving an *ee* value of approximately 35.5% at 30 °C (Fig. 11g).

Chiral 2,5-hexandiol (HDO) is another important precursor for chiral drugs and agricultural chemicals, which was successfully separated by chiral MOF membranes ((±)-[{Zn_2(cam)$_2$(dabco)}$_n$]).[84] The compatible size of HDO with pores of MOF and the hydrogen bond with Zn-carboxylate groups in MOF ensured the adsorption HDO by MOF. The separation of R-HDO and S-HDO was achieved by their different adsorption rate with ((±)- [{Zn_2(cam)$_2$(dabco)}$_n$]) membranes.

Most drugs are racemate with enantiomers, and generally only one enantiomer possesses therapeutic effects, while the other may be ineffective or cause side effects.[85] Yan et al. reported the CD-MOF MMMs for the separation of phenylalanine (Phe) enantiomers with 100% separation efficiency (Fig. 12a).[86] When the loads of CD-MOF in MMMs was 5%, the *ee* value reached the maximum (Fig. 12b). The *ee* was lower when the MOF loading was 3% as CD-MOF content was too low to provide sufficient chiral recognition sites. The separation performance at CD-MOF loading levels of 7% and 9% was also lower than that at loading level of 5%, due to the aggregation of CD-MOF in the membrane, which led to the generation of defects in membrane and decreased binding sites. The binding affinity between L-Phe and the chiral sites in CD-MOF was stronger, allowing it to adsorb in the membrane. While D-Phe did not interact with CD-MOF and preferentially passed through membrane to achieve chiral separation of Phe enantiomers.

In addition, chiral MOF membranes can also be used to separate naproxen to obtain *S*-naproxen with pain relief and anti-inflammatory effects.[23] Compared to *S*-naproxen, *R*-naproxen exhibited a

stronger affinity for interaction with chiral MOF-808. When enantiomers passed through the membrane, *R*-naproxen underwent noncovalent interaction with chiral MOF within the membrane while *S*-naproxen preferentially permeated through the membrane. The molecular dynamics simulation showed that there was almost no significant difference in the diffusion rates of the two enantiomers in MOF-808, while the diffusivity of *S*-naproxen in chiral MOF-808 was higher than that of *R*-naproxen. The chiral MOF-808-Ala obtained by *l*-Alanine (*l*-Ala) post modification showed an *ee* value of approximately 95.0%. Due to the excellent structural stability of chiral MOF-808, the membrane remained integrity after separation.

The separation of ibuprofen enantiomers is significant, as *S*-(+)-Ibuprofen is 160 times more pharmacologically active than *R*-(−)-ibuprofen and is more easily to be metabolized. Ben et al. prepared the chiral (*P*)-CoMOF membrane by symmetrical breaking in ligand dimethyl pyridine-2,5-dicarboxylate and cobalt ions.[87] Efficient separation of ibuprofen enantiomers (100% ee) was achieved, according to the different adsorption and desorption rates of *S*-(+)-ibuprofen and *R*-(−)-ibuprofen on (*P*)-CoMOF membrane.

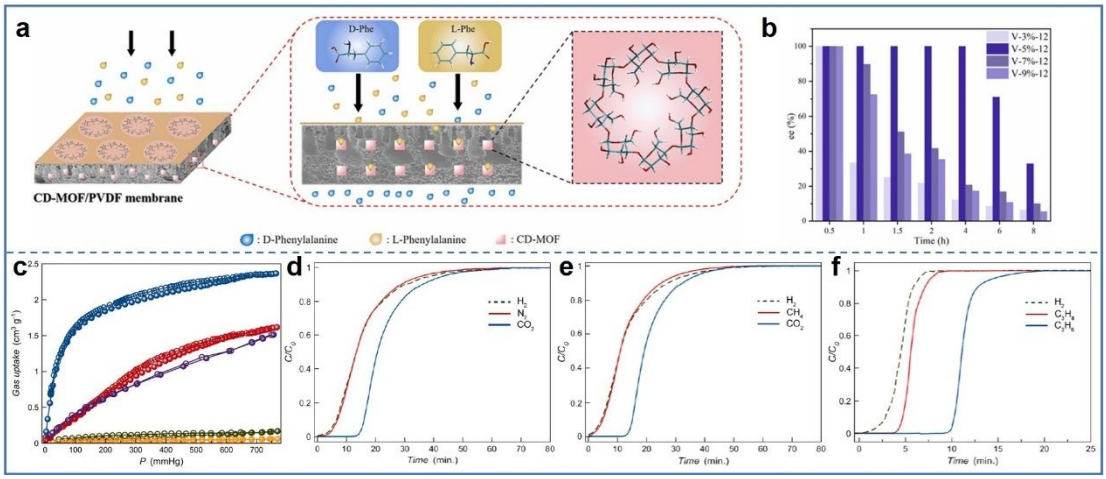

Fig. 12 (a) Schematic diagram of CD-MOF MMMs for separation of Phe enantiomers. (b) The *ee*% of Phe over the CD-MOF MMMs prepared with different CD-MOF loadings during the 8 h separation process. Reproduced with permission from ref. 86. Copyright 2023, Elsevier B.V. (c) The adsorption isotherms of C_3H_6, C_3H_8, CO_2, CH_4, and N_2 from top to bottom at 298 K for the activated Cu^{II}_2(*S*,*S*)-hismox·$5H_2O$. Experimental column breakthrough curves of (d) N_2/CO_2 (volume ratio was 75:25), (e) CH_4/CO_2 (volume ratio was 75:25), and (f) C_3H_6/C_3H_8 (volume ratio was 50:50) gas mixtures measured at 298 K and 1 bar. Reproduced with permission from ref. 89.

View Article Online
DOI: 10.1039/D5NR00938C

Chiral MOF membranes are also used for the separation of gas mixtures due to their differences in interactions with different gas molecules. Jin et al. prepared chiral $[Ni_2(mal)_2(bpy)]\cdot 2H_2O$ membrane for selective separation of H_2/CO_2.[88] The ideal selectivity of H_2/CO_2 was calculated to be 89 based on the permeability of the membrane to H_2 and CO_2. Due to the significant quadrupole moment and polarizability, the strong interaction between CO_2 and chiral MOF frameworks resulted in powerful adsorption onto the membrane. The lower permeability of CO_2 compared to H_2 caused excellent H_2/CO_2 separation selectivity of the chiral MOF membrane.

Pardo et al. achieved selective separation of gas mixtures including natural gas, flue gas, and petrochemical industrial gas via chiral MOF membrane.[89] The chiral Cu^{II}_2(*S*,*S*)-hismox$\cdot 5H_2O$ was dispersed into poly(ether-*co*-amide) multiblock copolymer to prepare the MMMs as the stationary phase for the chromatographic column, achieving the separation of CO_2/N_2, CO_2/CH_4, and C_3H_8/C_3H_6 gas mixtures. Chiral MOFs possessed significant adsorption capacity for CO_2, C_3H_8, and C_3H_6, but almost no adsorption capacity for CH_4 and N_2, indicating their potential for separating gas mixtures (Fig. 12c-f). The noninteracting channels were formed with MOFs, which preferentially passed through the membrane, consistent with the poor adsorption of CH_4 and N_2 by MOFs. This chiral MOF membrane enabled the separation of gas mixtures for economical or environmental values.

The separation of chiral drug precursors, drug molecules, and gas molecules has been achieved by chiral MOF membranes through distinguishable absorption or desorption rates of enantiomers from membranes. Compared to traditional chromatographic separation, chiral MOF membrane separation shows advantages of low energy consumption, easy adjustments of pore size and functional groups, and large-scale separation. Even though, more types of chiral MOF membranes with high quality are still needed to be developed for mechanical research, higher separation efficiency, and adaptability for more enantiomers.

3.3. Circular polarization luminescence

CPL refers to left-handed or right-handed circularly polarized luminescence, which has broad application prospects in fields such as 3D display, chiral recognition, information storage, and optoelectronic devices.[90] MOF materials are ideal chiral luminophores, as their specific porous

structures provide multiple routes for chiral emission, including chiral units on the MOF blocks and in the pores, so as the emissive units.[91]

Gu et al. encapsulated the lanthanide complexes $Ln(acac)_3$ (acac was acetylacetone) into the pores of chiral MOF $[Zn_2(cam)_2dabco]_n$ to obtain $Ln(acac)_3$@SURchirMOF membrane with excellent CPL property (Fig. 13a).[92] The lanthanide complexes $Eu(acac)_3$, $Tb(acac)_3$, and $Gd(acac)_3$ emitted primary red, green, and blue light under ultraviolet irradiation, respectively. The chiral MOFs with weak photoluminescent emission in the membrane hardly affected the photoluminescent emission of lanthanide complexes. MOFs kept chirality after the encapsulation of $Ln(acac)_3$, indicated from the same circular dichroism (CD) signals (Fig. 13c). The $Ln(acac)_3$@SURchirMOF membrane exhibited photoluminescent emission like that of $Ln(acac)_3$, thereby achieving tunable CPL of the membrane (Fig. 13d). The increase in fluorescent lifetime of chiral MOFs in the membrane and the decrease in fluorescent lifetime of lanthanide complexes indicated energy transfer from $Ln(acac)_3$ to chiral MOFs, where $Ln(acac)_3$ acted as the donor and chiral MOFs acted as the acceptor. The encapsulation of lanthanide complexes in chiral MOF pores was crucial for achieving CPL property, as the coordination or intermolecular interactions between acac in the complex and Zn nodes in the MOF resulted in efficient energy transfer (Fig. 13b).

Another method to endow MOF membranes with CPL properties is to encapsulate chiral molecules into luminescent MOF membranes. Zhang's group prepared luminescent MOF membrane using lbl spraying method and then loaded chiral molecules into the pores of MOFs to endow the membrane with CPL properties.[93] The aggregation-induced emission based molecule 4,4'-(1,2-diphenylethene-1,2-diyl) dibenzoic acid (TPE) was used as the ligand to self-assemble with Zn ions through lbl method, resulting in ZnTPE membrane with photoluminescence. Then, the chiral dibenzoyl-tartatic acid was loaded into the pores of ZnTPE through post modification method. The fluorescence emission of MOF membrane loaded with chiral molecules maintained strong fluorescence with a shift from 495 nm to 478 nm. The membrane exhibited uniform CPL signal due to the π-π conjugation effect between the benzene ring of the loaded chiral molecule and ZnTPE.

In addition, the same group also prepared the chiral D/L-ZnHF-SO_2 (HF-SO_2 was 3,7-Dibenzothiophenedicarboxylate, 5,5-dioxide) membranes using camphorsulfonic acid as a chiral inductor via the lbl chiral induction method (Fig. 13e).[94] The ZnHF-SO_2 membranes exhibited strong CPL properties with the CPL signal appearing at 440 nm, consistent with the fluorescent

emission of the membranes. The 9-fluororenone-2,7-dicarboxylate (HF-CO) molecule had a similar structure to the HF-SO_2 ligand in MOFs and therefore could be introduced as a mixed ligand to prepare photoluminescent MOFs. By adjusting the proportion of ligands, CPL colors in MOF membranes could be modulated (Fig. 13f). The membranes with different ligand ratios exhibited CPL signals at different positions due to energy transfer between HF-SO_2 ligands to Zn ions and Zn ions to HF-CO ligands.

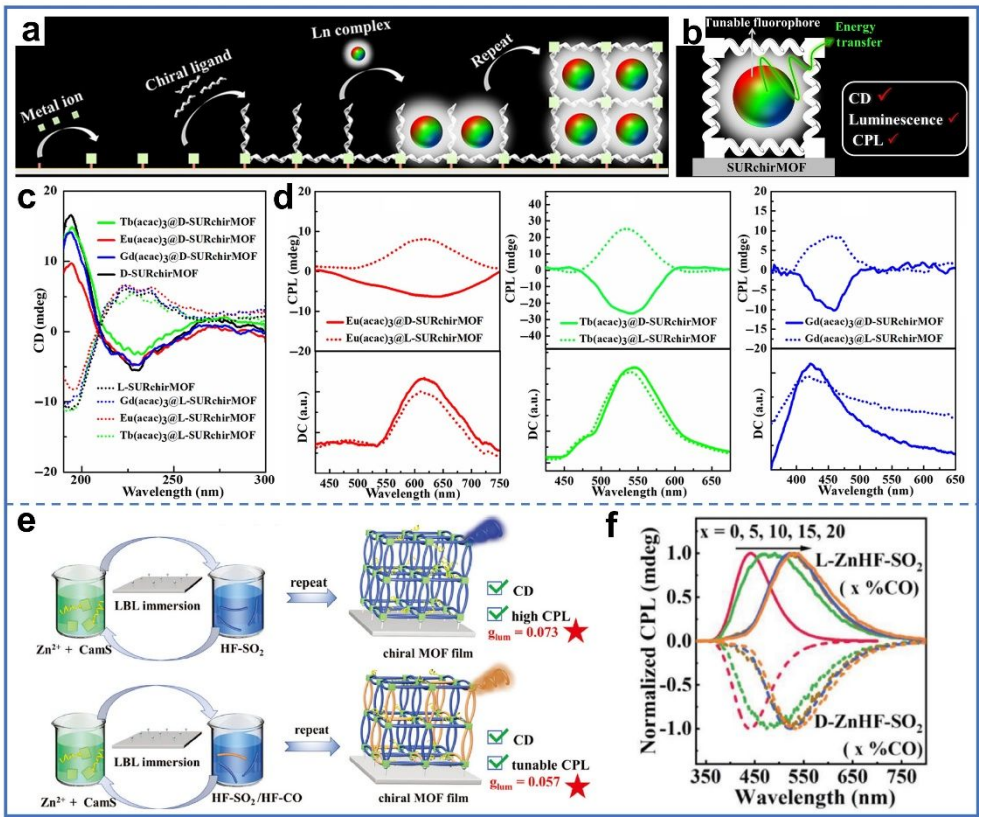

Fig. 13 (a) Schematic diagram of Ln(acac)$_3$@SURchirMOF membrane prepared by encapsulating Ln complex into chiral MOF pores. (b) Schematic diagram of energy transfer in the host–guest membrane of Ln(acac)$_3$@SURchirMOF. (c) The CD spectra of Ln(acac)$_3$@SURchirMOF and chiral MOF. (d) The CPL spectra of Ln(acac)$_3$@SURchirMOF. Reproduced with permission from ref. 92. Copyright 2022, Springer Nature. (e) Schematic diagram of the preparation of D/L-ZnHF-SO_2 membranes and tunable D/L-ZnHF-SO_2 membranes with mixed ligands by lbl chiral induction method. (f) The normalized CPL spectra of D/L-ZnHF-SO_2 (x% CO represented the proportion of HF-CO ligands) membranes. Reproduced with permission from ref. 94. Copyright 2024, Wiley-VCH.

Furthermore, Zhang's group crosslinked CLC with MOFs to prepare CLCMOF membrane for

achieving CPL performance in photo-thermal switching, which were used for information anticounterfeiting and encryption.[58] CLC was a thermally induced liquid crystal that gradually changed from an amorphous solid-like state to a transparent liquid state with increasing temperature, and the transmittance of the membrane also increased with increasing temperature. The UV–vis spectra of CLCMOF membrane are consistent with the CLC/MOF membrane loaded with CLC without cycloaddition reaction, indicating that CLCMOF membrane remained photochromic properties. The S-LCMOF membrane selectively reflected right-handed circularly polarized light and transmitted left-handed circularly polarized light, while R-LCMOF membrane was the opposite. When the membrane was heated at 140 °C and irradiated with UV, the CPL changed from yellow to blue fluorescence. Since the photoluminescence and CPL signals of CLCMOF membrane were regulated through irradiation and heating, molecular logic gates were designed for Morse code information encryption.

Chiral MOF membranes have been proven an ideal platform for CPL development due to their diverse structures and helical channels. Long-range periodic stacking in chiral MOF membranes is advantageous for the improvement of photoluminescence quantum yield and asymmetric factor. In addition, guest luminescent materials with different wavelength are easy to be encapsulated into chiral MOFs for colorful CPLs. In the future, organic ligands or metal ions with specific chiral centers and coordination geometries, respectively, are expected to be introduced for more efficient chiral transfer and CPL.

In Table 1, we summarized MOF materials and matrices used for chiral MOF membranes, as well as their applications.

Table 1 Compositions and applications of chiral MOF membranes

	MOF materials	Matrices	Applications
Pure chiral MOF membranes	Ni_2(*l*-asp)$_2$(bipy)		Separation of racemic MPD[27]
	l-His-ZIF-8		Separation of racemic 1-phenylethanol[19]
	MOF-808-Ala, MOF-808-Thr, MOF-808-His		Separation of racemic naproxen enantiomers[23]
	$Cu_2(DCam)_2(AzoBiPyB)$		Enantiopure uptakes of racemic phenylethanol[28]
	γCD-SURMOF		Recognition and separation of enantiomeric tripeptide pair[29]
	His-ZIF-8, $[Cd(LTP)_2]_n$,		Recognition of racemic

View Article Online
DOI: 10.1039/D5NR00938C

	[Cu(mal)bpy]·H_2O		phenylethanol, HAS, BSA, or INS[30]
	Meso-L-CuMOF		Recognition of monosaccharide enantiomers[64]
	Cu_2(DCam)$_2$(dabco), Cu_2(DCam)$_2$(BiPy), Cu_2(DCam)$_2$(BiPyB), HKUST-1, Cu(BDC), Cu(BPDC)		Recognition of limonene, 2-octanol, 1-phenylethanol, 1-phenylethylamine, or methyl lactate enantiomers[69]
	c-ZIF-8		Detection of Trp, Ala, and Leu enantiomers[76]
	Cu_2(*d*-cam)$_2$P		Separation of racemic 1-phenylethanol[82]
	Ni_2(*l*-asp)$_2$(bipy)		Separation of racemic MPD at low temperatures[83]
	[Ni_2(mal)$_2$(bpy)]·2H_2O		Separation of H_2/CO_2[88]
	Ln(acac)$_3$@SURchirMOF		CPL performance[92]
	ZnTPE		CPL luminescence performance[93]
	D/L-ZnHF-SO_2		CPL properties[94]
MMMs	RT@CDMOF	PES	Recognition of lactic acid enantiomers[25]
	MIL-53-NH-*l*-His	PES	Separation of racemic 1-phenylethanol[44]
	γ-CD-MOF	PES	Separation of racemic 1-phenylethanol[53]
	Zn-BLD	HDPE and UHMWPE	Separation of racemic methyl phenyl sulfoxide[55]
	Zn_2(sdc)$_2$	CLC	Information encryption of Morse code[58]
	D-Met@MOF	MPN	Anti-biofouling efficacy[59]
	[Cu_2((+)-Cam)$_2$Dabco]$_n$, [Cu_2((+)-Cam)$_2$Bipy]$_n$	Poly(dopamine) and polycarbonate trail etched membrane	Separation of racemic 1-phenylethanol[62]
	1-MONs	PES	Sensing of terpenes and terpenoids[38]
	L-His&R6G@ZIF-8	PVDF	Sensing of proline enantiomers[54]
	MOF nanofibers	CS	Electrochemical sensing of Tyr isomers[75]
	Eu(BTC)(H_2O)·DMF	PIM-1	Separation of 2-amino-1-butanol enantiomers[79]
	CD-MOF	PVDF	Separation of Phe enantiomers[86]
	Cu^{II}_2(*S*,*S*)-hismox·5H_2O	Poly(ether-co-amide) multiblock copolymer	Separation of CO_2/N_2, CO_2/CH_4, and C_3H_8/C_3H_6[89]

4. Conclusions and outlook

View Article Online
DOI: 10.1039/D5NR00938C

Chiral MOF membranes show great potential in chiral recognition or separation and chiral emission, due to the porous structure and simplicity of chiral functionalization. In this review, we first summarized the various methods to synthesize the chiral MOF membranes, including the direct methods for preparing pure chiral MOF membranes (eg. solvothermal synthesis, lbl synthesis, and template-assisted synthesis) and indirect methods for chiral MOF MMMs (eg. solution casting and TIPS-HoP. Pure chiral MOF membranes contain high density of functional sites, while MMMs exhibit excellent flexibility and stability.

Second, we summarized the applications of chiral MOF membranes in chiral sensing, separation, and CPL. Chiral MOF membranes have been applied in chiral sensing and separation for multiple molecules with high detectivity and selectivity. Membranes that combine photoluminescent units with chiral MOFs or chiral molecules with luminescent MOFs display tunable CPL, showing potential applications in imaging, optoelectronic devices, information anticounterfeiting and encryption.

However, the successful applications of chiral MOF membranes are still limited, which can be attributed to the difficulty in the fabrication of qualified membranes, even though the abundant chiral MOF materials. To improve the quality of the chiral MOF membranes, efforts could be made in the following aspects.

From the side of MOF materials, the exploration of functional groups, such as the groups with chirality or catalytic sites, is important to broaden the applications. Also, stable ligands and metal ions should be selected to improve the stability of chiral MOFs. Further, the synthesis method and conditions, such as the ratios between metal ions and organic ligands, should be creatively modified to optimize the size of MOF particles.

From the side of membranes, interface between MOF particles and matrix in MMMs is the main concern. To achieve the high-quality membranes (defect-free, uniform, and dense), the MOF materials should be compatible with the polymer matrix. Thus, functional groups on organic ligands in chiral MOFs and matrices should be carefully considered in covalent or coordination interactions. In addition, introducing specific functional groups, such as hydrophobic groups and corrosion-resistant groups, should be considered, to enhance water resistance and chemical stability. Furthermore, membrane preparation techniques should be broadened to provide better and multifunctional membranes, such as electrochemical deposition and microwave-assisted methods.

View Article Online
DOI: 10.1039/D5NR00938C

Chiral MOF membranes, as an emerging functional material, have shown great performance for chiral recognition and luminescence. With further improvement in the quality and functional investigation, chiral MOF membranes are expected to play a more important role in these fields.

Author contributions

Yun Fan conceived and wrote the manuscript. Mengyun Chen conceptualized and revised the review.

Conflicts of interest

The authors have declared no conflict of interest.

Data availability statements

No primary research results, software or code have been included, and no new data were generated or analyzed as part of this review.

Acknowledgements

This work was supported by the National Natural Science Foundation of China 22205100.

References

1. H. Furukawa, K. E. Cordova, M. O'Keeffe and O. M. Yaghi, *Science*, 2013, **341**, 1230444.
2. G. Lu, S. Li, Z. Guo, O. K. Farha, B. G. Hauser, X. Qi, Y. Wang, X. Wang, S. Han, X. Liu, J. S. DuChene, H. Zhang, Q. Zhang, X. Chen, J. Ma, S. C. J. Loo, W. D. Wei, Y. Yang, J. T. Hupp and F. Huo, *Nat. Chem.*, 2012, **4**, 310-316.
3. J. Guo, Y. Qin, Y. Zhu, X. Zhang, C. Long, M. Zhao and Z. Tang, *Chem. Soc. Rev.*, 2021, **50**, 5366-5396.
4. Q. Zhou, Q. Ding, Z. Geng, C. Hu, L. Yang, Z. Kan, B. Dong, M. Won, H. Song, L. Xu and J. S. Kim, *Nano-Micro Lett.*, 2025, **17**, 50.
5. J. He, X. Wen, L. Wu, H. Chen, J. Hu and X. Hou, *TrAC Trends Anal. Chem.*, 2022, **156**, 116715.
6. Z. Huang, X. Shen, Y. Wei, J. W. Chew, E. H. Ang and M. Pan, *Mater. Horiz.*, 2024, **11**, 6098-6106.
7. Y. Wang, N. Wu, Y. Wang, H. Ma, J. Zhang, L. Xu, M. K. Albolkany and B. Liu, *Nat. Commun.*, 2019, **10**, 2500.
8. Z. Liu, J. Ai, T. Bai, Y. Fang, K. Ding, Y. Duan, L. Han and S. Che, *Chem*, 2022, **8**, 186-196.

View Article Online
DOI: 10.1039/D5NR00938C

9. J. E. Rekoske, *AIChE J.*, 2001, **47**, 2-5.
10. D. S. Bradshaw, J. M. Leeder, M. M. Coles and D. L. Andrews, *Chem. Phys. Lett.*, 2015, **626**, 106-110.
11. X. Su, J. Sun, J. Liu, Y. Wang, J. Wang, W. Tang and J. Gong, *Angew. Chem. Int. Ed.*, 2024, **63**, e202402886.
12. N. Chhabra, M. L. Aseri and D. Padmanabhan, *Int. J. Appl. Basic Med. Res.*, 2013, **3**, 16-18.
13. C. D. Wu, A. Hu, L. Zhang and W. B. Lin, *J. Am. Chem. Soc.*, 2005, **127**, 8940-8941.
14. Z. Sharifzadeh, S. A. A. Razavi and A. Morsali, *Green Chem.*, 2023, **25**, 8661-8678.
15. M. Zhang, Z.-J. Pu, X.-L. Chen, X.-L. Gong, A.-X. Zhu and L.-M. Yuan, *Chem. Commun.*, 2013, **49**, 5201-5203.
16. Z. Gu, Y. Luo, X. Zhang, Z. Zhu, Y. Wang, T. Tang, S. Zhang and W. Zhang, *TrAC, Trends Anal. Chem.*, 2024, **179**, 117864.
17. H.-J. Choi and D.-Y. Koh, *Membranes*, 2022, **12**, 357.
18. T. Duerinck and J. F. M. Denayer, *Chem. Eng. Sci.*, 2015, **124**, 179-187.
19. J. Y. Chan, H. Zhang, Y. Nolvachai, Y. Hu, H. Zhu, M. Forsyth, Q. Gu, D. E. Hoke, X. Zhang, P. J. Marriot and H. Wang, *Angew. Chem. Int. Ed.*, 2018, **57**, 17130-17134.
20. J. Liang, Y. Song, H. Xing, L. Ma, F. Wang, M. Zhang, H. Zhang, G. Zou and G. Yang, *Nanoscale*, 2024, **16**, 22011-22020.
21. Y.-H. Xiao, Z.-Z. Ma, X.-X. Yang, D.-S. Li, Z.-G. Gu and J. Zhang, *ACS Nano*, 2023, **17**, 19136-19143.
22. W. Wang, X. Dong, J. Nan, W. Jin, Z. Hu, Y. Chen and J. Jiang, *Chem. Commun.*, 2012, **48**, 7022-7024.
23. T. Chen, H. Li, X. Shi, J. Imbrogno and D. Zhao, *J. Am. Chem. Soc.*, 2024, **146**, 14433-14438.
24. H.-J. Choi, Y.-H. Ahn and D.-Y. Koh, *Membranes*, 2021, **11**, 279.
25. X.-L. Yang, Z.-Y. Yang, R. Shao, R.-F. Guan, S.-L. Dong and M.-H. Xie, *Adv. Mater.*, 2023, **35**, 2304046.
26. J. He, J. He, L. Tang, Y. Xia, J. Zhou, X. Jiang and X. Hou, *TrAC Trends Anal. Chem.*, 2024, **175**, 117709.
27. Z. Kang, M. Xue, L. Fan, J. Ding, L. Guo, L. Gao and S. Qiu, *Chem. Commun.*, 2013, **49**, 10569-10571.
28. A. B. Kanj, J. Buerck, S. Grosjean, S. Braese and L. Heinke, *Chem. Commun.*, 2019, **55**, 8776-8779.
29. L.-M. Chang, Q.-h. Li, P. Weidler, Z.-G. Gu, C. Wöll and J. Zhang, *CCS Chem.*, 2022, **4**, 3472-3481.
30. J. Yang, Q. Song, T. Zhang, Y. Yan, C. Yuan, Y. Cui and X. Hou, *Anal. Chem.*, 2024, **96**, 17280-17289.
31. X. Liang, F. Zhang, W. Feng, X. Zou, C. Zhao, H. Na, C. Liu, F. Sun and G. Zhu, *Chem. Sci.*, 2013, **4**, 983-992.
32. L. A. Hall, D. M. D'Alessandro and G. Lakhwani, *Chem. Soc. Rev.*, 2023, **52**, 3567-3590.
33. M. Ma, J. Chen, H. Liu, Z. Huang, F. Huang, Q. Li and Y. Xu, *Nanoscale*, 2022, **14**, 13405-13427.
34. Z. F. Chen, J. Zhang, R. G. Xiong and X. Z. You, *Inorg. Chem. Commun.*, 2000, **3**, 493-

View Article Online
DOI: 10.1039/D5NR00938C

496.

35. N. Corella-Ochoa, J. B. Tapia, H. N. Rubin, V. Lillo, J. González-Cobos, J. Luis Núñez-Rico, S. R. G. Balestra, N. Almora-Barrios, M. Lledós, A. Güell-Bara, J. Cabezas-Giménez, E. C. Escudero-Adán, A. Vidal-Ferran, S. Calero, M. Reynolds, C. Martí-Gastaldo and J. Ramón Galán-Mascarós, *J. Am. Chem. Soc.*, 2019, **141**, 14306-14316.
36. M. P. Yutkin, M. S. Zavakhina, D. G. Samsonenko, D. N. Dybtsev and V. P. Fedin, *Inorg. Chim. Acta*, 2013, **394**, 367-372.
37. K. Tanaka, D. Yanamoto, K. Yoshimura, T. Anami and Z. Urbanczyk-Lipkowska, *CrystEngComm*, 2015, **17**, 1291-1295.
38. Y. Liu, L. Liu, X. Chen, Y. Liu, Y. Han and Y. Cui, *J. Am. Chem. Soc.*, 2021, **143**, 3509-3518.
39. K. Berijani and A. Morsali, *J. Catal.*, 2019, **378**, 28-35.
40. P. Cui, P. Wang, Y. Zhao and W.-Y. Sun, *Cryst. Growth Des.*, 2019, **19**, 1454-1470.
41. Z. Han, K. Wang, Y. Guo, W. Chen, J. Zhang, X. Zhang, G. Siligardi, S. Yang, Z. Zhou, P. Sun, W. Shi and P. Cheng, *Nat. Commun.*, 2019, **10**, 5117.
42. W.-T. Kou, C.-X. Yang and X.-P. Yan, *J. Mater. Chem. A*, 2018, **6**, 17861-17866.
43. G. Yang, W. Shi, Y. Qian, X. Zheng, Z. Meng and H.-L. Jiang, *Angew. Chem. Int. Ed.*, 2023, **62**, e202308089.
44. Y. Lu, H. Zhang, J. Y. Chan, R. Ou, H. Zhu, M. Forsyth, E. M. Marijanovic, C. M. Doherty, P. J. Marriott, M. M. B. Holl and H. Wang, *Angew. Chem. Int. Ed.*, 2019, **58**, 16928-16935.
45. C. Tan, X. Han, Z. Li, Y. Liu and Y. Cui, *J. Am. Chem. Soc.*, 2018, **140**, 16229-16236.
46. B. Vilhanová, M. Ranocchiari and J. A. van Bokhoven, *ChemCatChem*, 2016, **8**, 308-312.
47. A. B. Kanj, J. Buerck, N. Vankova, C. Li, D. Mutruc, A. Chandresh, S. Hecht, T. Heine and L. Heinke, *J. Am. Chem. Soc.*, 2021, **143**, 7059-7068.
48. J.-S. Feng, M. Ren, Z.-S. Cai, K. Fan, S.-S. Bao and L.-M. Zheng, *Chem. Commun.*, 2016, **52**, 6877-6880.
49. T. Yamada, T. Eguchi, T. Wakiyama, T. Narushima, H. Okamoto and N. Kimizuka, *Chem. Eur. J.*, 2019, **25**, 6698-6702.
50. S.-T. Wu, Z.-W. Cai, Q.-Y. Ye, C.-H. Weng, X.-H. Huang, X.-L. Hu, C.-C. Huang and N.-F. Zhuang, *Angew. Chem. Int. Ed.*, 2014, **53**, 12860-12864.
51. J. Zhang, S. Chen, R. A. Nieto, T. Wu, P. Feng and X. Bu, *Angew. Chem. Int. Ed.*, 2010, **49**, 1267-1270.
52. D. Wu, K. Zhou, J. Tian, C. Liu, J. Tian, F. Jiang, D. Yuan, J. Zhang, Q. Chen and M. Hong, *Angew. Chem. Int. Ed.*, 2021, **60**, 3087-3094.
53. Y. Lu, J. Y. Chan, H. Zhang, X. Li, Y. Nolvachai, P. J. Marriott, X. Zhang, G. P. Simon, M. M. B. Holl and H. Wang, *J. Membr. Sci.*, 2021, **620**, 118956.
54. Y.-H. Geng, Y. Xin, J. Du, M.-Y. Cui, Y.-Y. Liu, L.-X. Zhang and B. Ding, *Spectrochim. Acta, Part A*, 2024, **305**, 123468.
55. H. Wang, S. Zhao, Y. Liu, R. Yao, X. Wang, Y. Cao, D. Ma, M. Zou, A. Cao, X. Feng and B. Wang, *Nat. Commun.*, 2019, **10**, 4204.
56. B. D. Freeman, *Macromolecules*, 1999, **32**, 375-380.
57. L. M. Robeson, *J. Membr. Sci.*, 2008, **320**, 390-400.
58. X.-X. Yang, N. Li, C. Li, Z.-B. Jin, Z.-Z. Ma, Z.-G. Gu and J. Zhang, *J. Am. Chem. Soc.*, 2024, **146**, 16213-16221.

59. Z. Yu, X. Li, Z. Wang, Y. Fan, W. Zhao, D. Li, D. Xu, T. Gu and F. Wang, *Adv. Mater.*, 2024, **36**, 2407409.
60. C. Li and L. Heinke, *Symmetry*, 2020, **12**, 686.
61. X. Niu, M. Yuan, X. Yang, H. Li, R. Zhao, Y. Liu, H. Zhao and K. Wang, *ACS Appl. Nano Mater.*, 2024, **7**, 19175-19183.
62. M. Chen, X. Li, J. Li, C. Liu, A. Yu and S. Zhang, *Sep. Purif. Technol.*, 2024, **331**, 125704.
63. L. Geng, Y. Qiao, R. Sun, L. Guo, Z.-Q. Li, Y. Ma, M.-H. Yu, Z. Chang and X.-H. Bu, *Adv. Mater.*, 2025, **37**, 2415511.
64. J. Guo, X. Liu, J. Zhao, H. Xu, Z. Gao, Z.-Q. Wu and Y.-Y. Song, *Chem. Sci.*, 2023, **14**, 1742-1751.
65. X. Niu, R. Zhao, Y. Liu, M. Yuan, H. Zhao, H. Li, X. Yang, H. Xu and K. Wang, *J. Mater. Chem. A*, 2023, **11**, 23376-23386.
66. J.-Y. Liu, Y.-H. Geng, T.-T. Wang, B. Ding, Y.-H. Qiao, J.-Z. Huo and B. Ding, *ACS Appl. Nano Mater.*, 2023, **6**, 398-409.
67. Y.-W. Zhao, L.-E. Guo, F.-Q. Zhang, J. Yao and X.-M. Zhang, *ACS Appl. Mater. Interfaces*, 2021, **13**, 20821-20829.
68. Y. Zhang, Y. Wang, Y. Dai, X. Bai, X. Hu, L. Du, H. Hu, X. Yang, D. Li, Q. Dai, T. Hasan and Z. Sun, *Sci. Adv.*, 2022, **8**, eabq8246.
69. S. Okur, P. Qin, A. Chandresh, C. Li, Z. Zhang, U. Lemmer and L. Heinke, *Angew. Chem. Int. Ed.*, 2021, **60**, 3566-3571.
70. P. Qin, B. A. Day, S. Okur, C. Li, A. Chandresh, C. E. Wilmer and L. Heinke, *ACS Sens.*, 2022, **7**, 1666-1675.
71. N. Li, J.-B. Zhang, C. Woell, Z.-G. Gu and J. Zhang, *Adv. Funct. Mater.*, 2025, 2422860.
72. L. Lan, X. Kuang, X. Sun, Q. Wei and R. Kuang, *Anal. Chem.*, 2023, **95**, 18295-18302.
73. X. Niu, S. Yan, R. Zhao, H. Li, X. Liu and K. Wang, *ACS Appl. Mater. Interfaces*, 2023, **15**, 22435-22444.
74 X. Niu, Y. Liu, R. Zhao, M. Yuan, H. Zhao, H. Li and K. Wang, *ACS Appl. Mater. Interfaces*, 2024, **16**, 17361-17370.
75. L. Tong, X. Kuang, Q. Duan and X. Zheng, *Starch-Stärke*, 2021, **73**, 2100112.
76. M.-Y. Wu, R.-J. Mo, X.-L. Ding, L.-Q. Huang, Z.-Q. Li and X.-H. Xia, *Small*, 2023, **19**, 2301460.
77. F. Wang, K. He, R. Wang, H. Ma, P. J. Marriott, M. R. Hill, G. P. Simon, M. M. B. Holl and H. Wang, *Adv. Mater.*, 2024, **36**, 2400709.
78. G. Sun, Y. Luo, Z. Yan, H. Qiu and W. Tang, *Chin. Chem. Lett.*, 2024, **35**, 109787.
79. S. Das, S. Xu, T. Ben and S. Qiu, *Angew. Chem. Int. Ed.*, 2018, **57**, 8629-8633.
80. Y. Duan, L. Li, Z. Shen, J. Cheng and K. He, *Membranes*, 2023, **13**, 480.
81. Z.-J. Li, J. Yao, Q. Tao, L. Jiang and T.-B. Lu, *Inorg. Chem.*, 2013, **52**, 11694-11696.
82. Z.-G. Gu, W.-Q. Fu, X. Wu and J. Zhang, *Chem. Commun.*, 2016, **52**, 772-775.
83. K. Huang, X. Dong, R. Ren and W. Jin, *AIChE J.*, 2013, **59**, 4364-4372.
84. B. Liu, O. Shekhah, H. K. Arslan, J. Liu, C. Woell and R. A. Fischer, *Angew. Chem. Int. Ed.*, 2012, **51**, 807-810.
85. F. Zhang, L. He, W. Sun, Y. Cheng, J. Liu and Z. Ren, *RSC Adv.*, 2015, **5**, 41729-41735.
86. Q. Ye, J. Li, Y. Huang, H. Wu, Y. Li and B. Yan, *J. Environ. Chem. Eng.*, 2023, **11**, 109250.
87. B. Li, Y. Feng, D. Zhou, M. Yang, D. Li, S. Zhang, J. Fu and T. Ben, *J. Mater. Chem. A*,

View Article Online
DOI: 10.1039/D5NR00938C

2025, **13**, 8375-8384.

88. Q. Li, G. Liu, K. Huang, J. Duan and W. Jin, *Asia-Pac. J. Chem. Eng.*, 2016, **11**, 60-69.
89. M. Mon, R. Bruno, E. Tiburcio, A. Grau-Atienza, A. Sepúlveda-Escribano, E. V. Ramos-Fernandez, A. Fuoco, E. Esposito, M. Monteleone, J. C. Jansen, J. Cano, J. Ferrando-Soria, D. Armentano and E. Pardo, *Chem. Mater.*, 2019, **31**, 5856-5866.
90. Y. Zhou, Y. Wang, Y. Song, S. Zhao, M. Zhang, G. Li, Q. Guo, Z. Tong, Z. Li, S. Jin, H.-B. Yao, M. Zhu and T. Zhuang, *Nat. Commun.*, 2024, **15**, 251.
91. C. Li, H. Schopmans, L. Langer, S. Marschner, A. Chandresh, J. Buerck, Y. Tsuchiya, A. Chihaya, W. Wenzel, S. Braese, M. Kozlowska and L. Heinke, *Angew. Chem. Int. Ed.*, 2023, **62**, e202217377.
92. R. Zhai, Y. Xiao, Z. Gu and J. Zhang, *Nano Res.*, 2022, **15**, 1102-1108.
93. X.-X. Yang, C. Li, S.-M. Chen, Z.-G. Gu and J. Zhang, *Chem. Eur. J.*, 2024, **30**, e202400350.
94. C. Li, X.-X. Yang, M.-Y. Zheng, Z.-G. Gu and J. Zhang, *Adv. Funct. Mater.*, 2024, **34**, 2401102.

View Article Online
DOI: 10.1039/D5NR00938C

Data availability statements

No primary research results, software or code have been included, and no new data were generated or analyzed as part of this review.